1972

Radiolysis of tris (ethylenediamine) cobalt (III) salts

David Witiak
Iowa State University

INFORMATION TO USERS

This dissertation was produced from a microfilm copy of the original document. While the most advanced technological means to photograph and reproduce this document have been used, the quality is heavily dependent upon the quality of the original submitted.

The following explanation of techniques is provided to help you understand markings or patterns which may appear on this reproduction.

1. The sign or "target" for pages apparently lacking from the document photographed is "Missing Page(s)". If it was possible to obtain the missing page(s) or section, they are spliced into the film along with adjacent pages. This may have necessitated cutting thru an image and duplicating adjacent pages to insure you complete continuity.

2. When an image on the film is obliterated with a large round black mark, it is an indication that the photographer suspected that the copy may have moved during exposure and thus cause a blurred image. You will find a good image of the page in the adjacent frame.

3. When a map, drawing or chart, etc., was part of the material being photographed the photographer followed a definite method in "sectioning" the material. It is customary to begin photoing at the upper left hand corner of a large sheet and to continue photoing from left to right in equal sections with a small overlap. If necessary, sectioning is continued again — beginning below the first row and continuing on until complete.

4. The majority of users indicate that the textual content is of greatest value, however, a somewhat higher quality reproduction could be made from "photographs" if essential to the understanding of the dissertation. Silver prints of "photographs" may be ordered at additional charge by writing the Order Department, giving the catalog number, title, author and specific pages you wish reproduced.

University Microfilms

300 North Zeeb Road
Ann Arbor, Michigan 48106

A Xerox Education Company

Radiolysis of tris(ethylenediamine)cobalt(III) salts

by

David Witiak

A Dissertation Submitted to the
Graduate Faculty in Partial Fulfillment of
The Requirements for the Degree of
DOCTOR OF PHILOSOPHY
Department: Chemistry
Major: Physical Chemistry

Approved:

Signature was redacted for privacy.

In Charge of Major Work

Signature was redacted for privacy.

For the Major Department

Signature was redacted for privacy.

For the Graduate College

Iowa State University
Ames, Iowa

1972

TABLE OF CONTENTS

I. INTRODUCTION

This dissertation is mainly a preliminary exploration of the effects radiation has on the optical isomers of the coordination compounds $[Co(en)_3]X_3$ (where X = Cl^-, Br^-, I^- and NO_3^-). In the course of the investigation it was necessary for the compounds to come in contact with elevated temperatures (about 60-80°C), from contact with the X-ray unit. Therefore the effects of temperature on the racemization was studied. In order to account for some of the effects observed in the thermal racemization data, the crystal structure of the nitrate complex was determined.

In addition to the above mentioned sources of radiation (i.e. thermal heat and X-rays), the complex was also subjected to irradiation with gamma-rays. The gamma-ray work was done only superficially and could provide a good topic for further consideration.

A. Optical Rotatory Dispersion and Circular Dichroism

Optical activity is the ability of a medium to rotate the plane of polarization of linearly polarized light. In order to have this ability, the medium must possess one or both of the following two criteria: macroscopic anisotropy or molecular dissymmetry. Macroscopic anisotropy may be due to the spacial arrangement of the molecules or to the influence of an external field. The requirements for molecular dissymmetry are that the medium not have:

a) a center of symmetry

b) a mirror plane

c) an improper axis.

The study of circular dichroism (CD) is accomplished by alternately passing right and left circularly polarized light components through the sample with a measurement of the absorption by the two components. In the study of optical rotatory dispersion (ORD) a beam of polarized light is passed through the sample and the angle of rotation is recorded.

The polarized light is produced (Figure 1) by passing light through a polarizing prism, (i.e. a Rochon prism, made of quartz) where it is polarized in one plane. As plane polarized light is passed through an optically active medium, the plane is rotated by an angle α. In order to have the minimum intensity of plane polarized light reach the detector, an analyzer prism, crossed to the polarizer, must be rotated either to the right or left by an angle which is equal to the rotation caused by the sample. This enables one to measure the direction and magnitude of the rotation experimentally.

In circular dichroism the plane of polarized light is passed through a Pockel's cell, made of ammonium dihydrogen phosphate, connected to an alternating electric potential which causes the plane polarized light to become alternately left and right circularly polarized light.

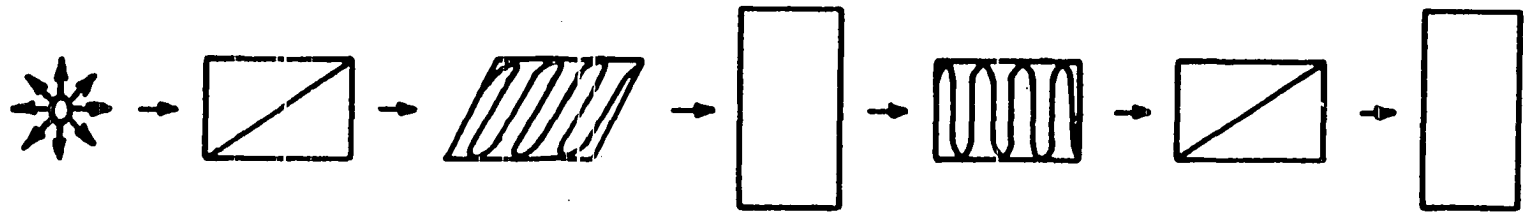

Figure 1. Block diagram of optical rotatory dispersion instrument

Plane polarized light passing through an optically active medium corresponds to two equally superimposed right and left circularly polarized components (Figure 2) designated by the letters D and L. Therefore we will have to consider two indices of refraction n_D and n_L and also two molar extinction coefficients ε_D and ε_L. These properties need not be different but at most wavelengths they are.

The combination of unequal absorption (circular dichroism) and unequal refractive indices (optical rotation) in the region in which optically active absorption bands are observed is called the Cotton Effect. It results in the appearance of an "anomalous" optical rotatory dispersion curve and in the appearance of a positive or negative circular dichroism curve. A positive Cotton Effect is described as having the tail of the effect remain positive while approaching longer wavelengths.

Specific rotation, as used in this dissertation, is dependent on the magnitude of the rotation caused by the optically active sample, the path length, l, of the light through the cell and also upon the concentration, c, of the optically active sample in a particular solvent.

The above terms are related by the following expression:

$$[\alpha]_\lambda = \alpha/lc$$

α = degrees measured

l = path length in decimeters

c = concentration in g/ml

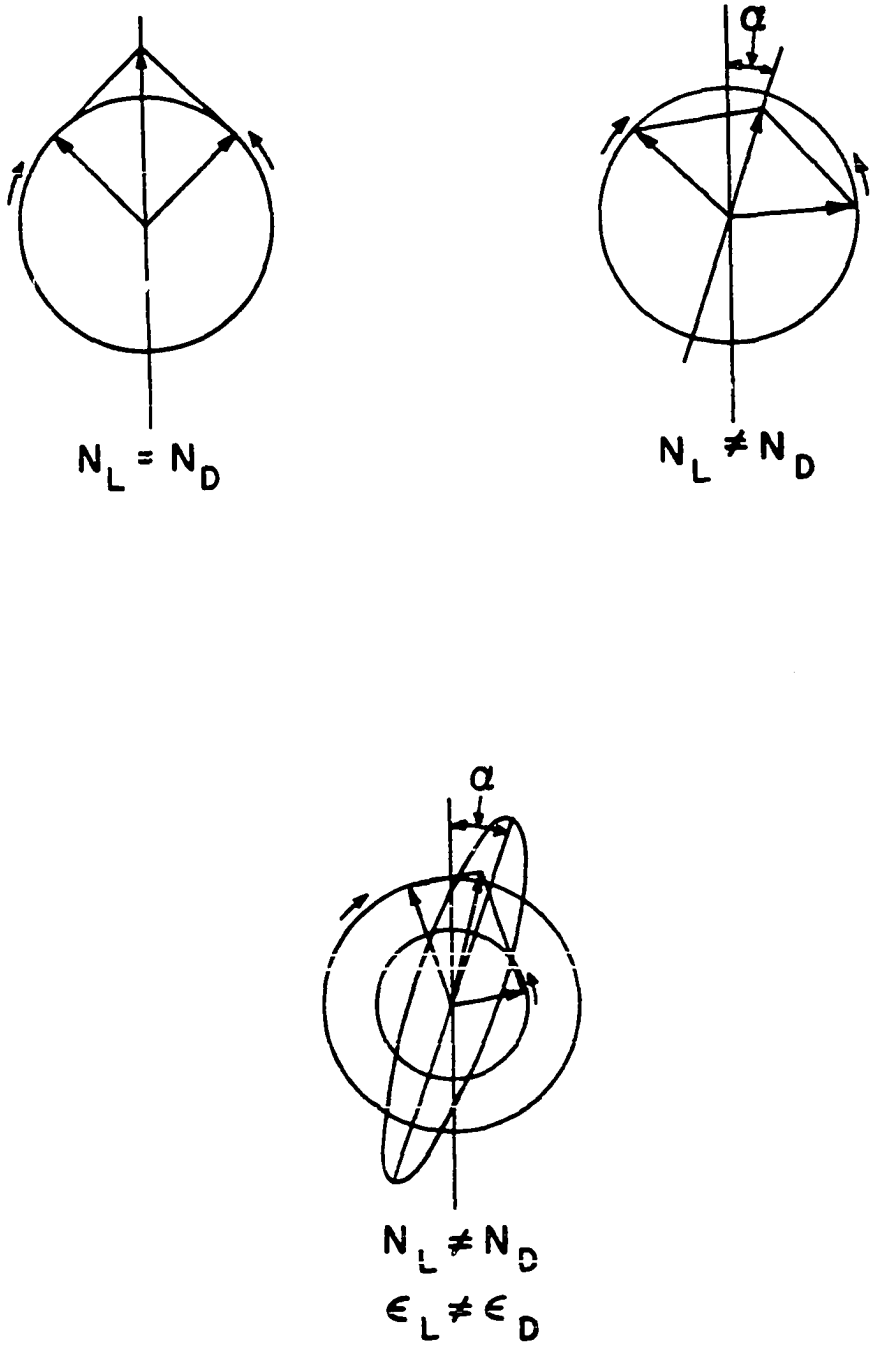

Figure 2. Cross sections of a non-absorbing optically active material showing vibration forms resolved into circularly polarized components

The circular dichroism, or the difference in molar extinction coefficients for right and left circularly polarized light, is defined as:

$\Delta\varepsilon = \Delta A/lc$ ΔA = measured absorbance difference

l = path length in centimeters

c = molar concentration

B. Absolute Configuration and Mechanisms for Racemization

The designations of absolute configurations are those of Piper (1) and redefined by Jensen (2). The structure which conforms to a left-handed helix is designated Λ and the mirror image or right-handed helix is designated Δ. The helical axis is taken as the threefold rotation axis. The isomer of $[Co(en)_3]^{3+}$ which has been designated as D, d or (+) in the literature corresponds to the Λ helix. In this dissertation the absolute configurations will be either designated by the Λ or D and Δ or L symbols and (+) or (-) will be used to describe the sign of the optical activity and will be associated with a particular wavelength. (Positive is a clockwise rotation of the plane of polarization as viewed by an observer from the source).

Two earlier mechanisms for molecular rearrangement leading to racemization of octahedral complexes that do not involve bond rupture have been proposed, one by Ray and Dutt (3) and the other by Bailar (4). The mechanism proposed by Bailar was also independently proposed by Gehman (5) and by

Seiden (6). The Ray and Dutt twist is shown in Figure 3a. By holding one of the rings fixed, the motion of the other two rings can be described by rotating them 90° in opposite directions about an axis perpendicular to their respective planes and passing through the metal ion. Throughout the twisting process the rings remain rigid, also the ligand-metal-ligand bond angles of a ring remain constant at approximately 90°.

In Figure 3b is pictured the Bailar twist as viewed down the C_3 axis. The racemization process may be described by rotating the three metal-ligand bonds (connected by the triangle) 120° about the C_3 axis in a counterclockwise direction. In the transition state there is a distortion of the chelate rings caused by the contraction of the ligand-metal-ligand bond angles. If all the ligand-metal-ligand bond angles are the same, in the transition state, the value would be 81°48'. Eisenberg and Ibers (7) completed the crystal structure of the trigonal prismatic compound $Re(S_2C_2(C_6H_5)_2)_3$ which had chelate ring angles of 81.9°, 81.5° and 80.9°.

Springer and Sievers (8) recently proposed a new mechanism as shown in Figure 3c. In this twist, as in the Ray and Dutt mechanism, one chelate ring is fixed while the other two rotate. The difference between the two mechanisms is that instead of the two chelate rings rotating past each other in their own planes they rotate while continually changing

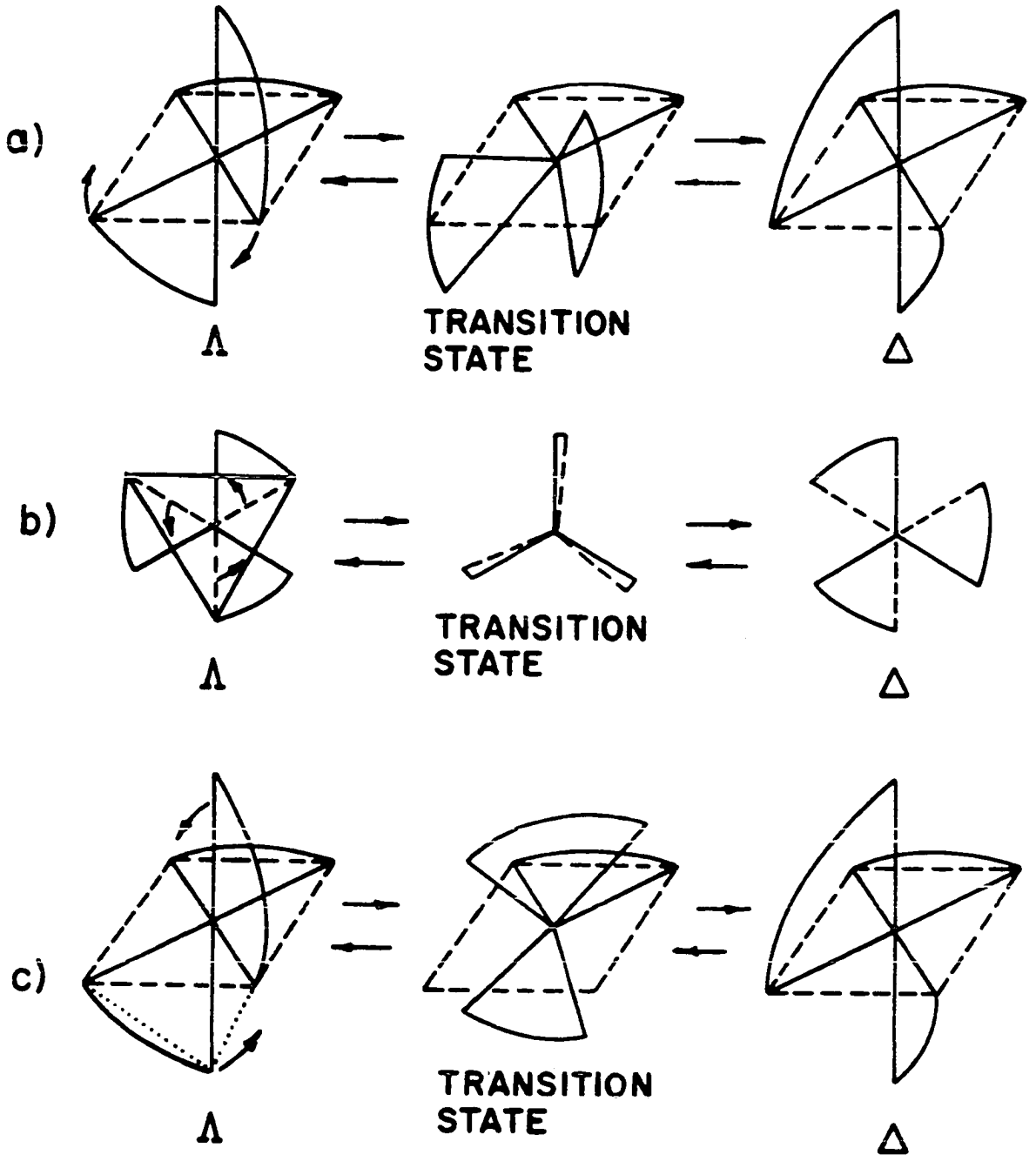

Figure 3. Proposed intramolecular mechanisms for optical isomerization of a tris octahedral complex with bidentate ligands
(a) Ray and Dutt
(b) Bailar
(c) Springer and Sievers

planes. The process can be described as a rotation of 120° by each ring about an axis coming out of a face of the octahedron (dotted lines, the same being true for the other chelate ring).

The Springer and Sievers twist is a special case of the Bailar twist. The difference between the two mechanisms is that in the Bailar twist all ligand-metal-ligand bond angles are free to change while in the Springer and Sievers twist particular bond angles within a ring are held constant. The Springer and Sievers mechanism produces a transition state similar to that of the Bailar twist about the real C_3 axis of the molecule.

The actual racemization process of a chelate complex by a twist mechanism probably lies somewhere between the ideal Bailar mechanism, having all acute ligand-metal-ligand bond angles equal to 81°48' in the transition state and that of the rigid-ring mechanisms having the angles 90° between one arm of the fixed ligand and the rotating ligand, in the transition state. The preference for either mechanism would probably depend on the strength of the ligand-metal bond and upon the bulkiness of the substituents on the metal.

C. Electronic Transition States

Transition metal coordination complexes are, in general, sensitive to ultraviolet or visible light and may react under the influence of this light to form new chemical species.

Many different photochemical reactions have been observed for coordination complexes, some examples include: oxidation-reduction, ligand exchange, geometrical or optical isomerization or simply decomposition. Until recently, the study of inorganic photochemistry has not been a popular area; several factors have attributed to this slow progress. Among there are: inadequacies in the description of bonding and the energy levels in many coordination complexes, the sketchy understanding of the thermal chemistry of these systems and frequently the complexity of the photochemical reactions themselves.

In order to have a better understanding of the chemical processes in coordination complexes a knowledge of the bonding and energy levels is desirable. The complexes of cobalt(III) contain six metal-ligand sigma bonds and may be considered to have octahedral or pseudo-octahedral symmetry. In constructing molecular orbitals for an octahedral system, nine valence shell orbitals of the metal are to be considered: six of the orbitals {d(z^2), d($x^2 - y^2$) [having e_g symmetry], s [having a_{1g} symmetry] and p(x), p(y) and p(z) [having t_{1u} symmetry]} have their lobes lying along the metal-to-ligand axes and are used in the formation of sigma bonds. The other three metal orbitals {d(xy), d(yz) and d(xz) [having t_{2g} symmetry]} are only available for pi bonding if the ligand has suitable pi orbitals. Each of the

bonding metal orbitals combine with corresponding ligand LCAO's to form six sigma bonding and six antibonding molecular orbitals. A diagram showing the construction of the molecular orbitals for a sigma-bonded complex containing ligands with no available pi orbitals is given in Figure 4. In $[Co(en)_3]^{3+}$ there is wide separation between the t_{2g} and the e_g* orbitals (the strong ligand field situation). The twelve nitrogen lone-pair electrons are used to fill the lower six available bonding molecular orbitals {3-t_{1u}, 1-a_{2g} and 2-e_g orbitals}. The six d-electrons, from the metal, are located in the non-bonding t_{2g} orbitals. Because the t_{2g} orbitals are filled with all electrons paired, the electronic configuration is described by the totally symmetric term symbol $^1A_{1g}$. The superscript, one, preceding the letter A designates a singlet ground-state (i.e. all the electrons are paired, the multiplicity is equal to 2S + 1, where S is the spin quantum number).

In most strong field d^6 octahedral complexes, the lowest singlet-singlet energy transition from the ground state is magnetic dipole allowed, whereas the spin forbidden and many of the higher energy ligand field transitions are both magnetic and electric dipole forbidden. The criterion used for determining if a transition is allowed or forbidden is given in the following:

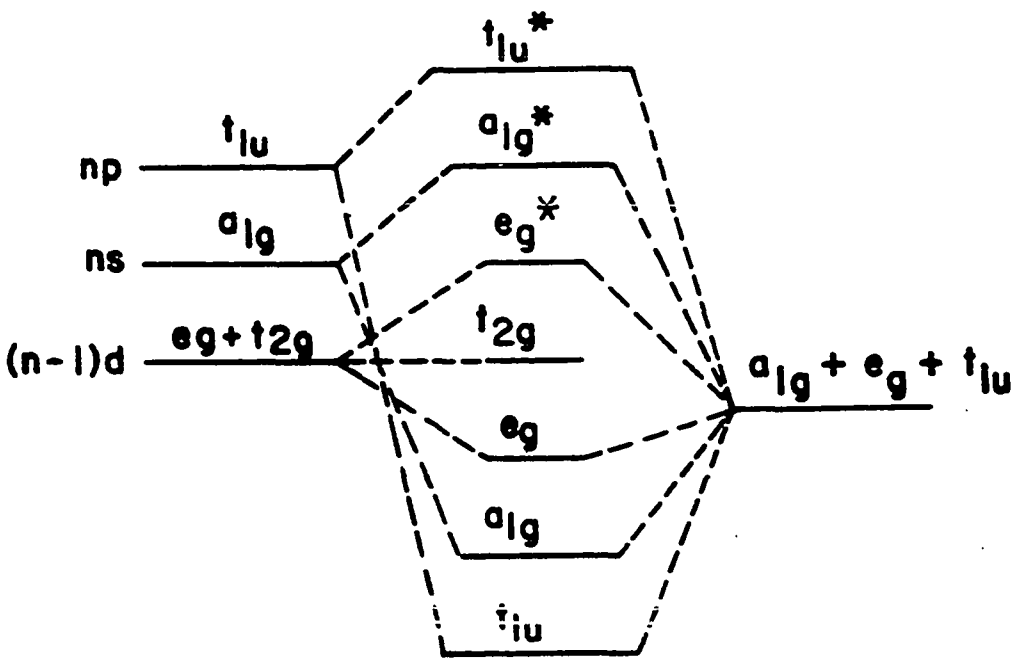

Figure 4. Construction of molecular orbitals for octahedral coordination complexes of non pi-bonding ligands utilizing metal nd orbitals

a) For electrically allowed transitions

$\underline{U}|\bar{O}|\underline{V}$ contains the Γ_1 or totally symmetric representation. Where $\underline{U}$ and $\underline{V}$ represent the initial and final state wavefunctions, respectively. $|\bar{O}|$ is the electric dipole operator and is a basis for the symmetry representations of $\underline{x}$, $\underline{y}$ and $\underline{z}$.

b) For magnetically allowed transitions

$\underline{U}|\bar{O}|\underline{V}$ contains the Γ_1 or totally symmetric representation. where $\underline{U}$ and $\underline{V}$ have the same definition as above and the operator $|\bar{O}|$ belongs to the symmetry representations for $R\underline{x}$, $R\underline{y}$ and $R\underline{z}$.

For a transition to be optically active (i.e. have the properties of non-zero "anomalous" optical rotatory dispersion and circular dichroism) the product of the integrals of terms in (a) and (b) must be non-zero. Therefore each integral has to be non-zero. As an example for cobalt(III) in an octahedral field the: $^1A_{1g} \rightarrow {}^1T_{1g}$ and $^1A_{1g} \rightarrow {}^1T_{2g}$ are both electric dipole forbidden transitions, whereas the $^1A_g \rightarrow {}^1T_{1g}$ is magnetically allowed and the $^1A_{1g} \rightarrow {}^1T_{2g}$ is magnetically forbidden. In true octahedral complexes there is no optical activity.

The actual point group of the $[Co(en)_3]^{3+}$ cation is D_3 and the degeneracies of the lower $^1T_{1g}$ and higher $^1T_{2g}$ electronic states are reduced into (Figure 5): $^1A_2 + {}^1E_a$ and $^1A_1 + {}^1E_b$ components, respectively. The transition from the ground-state to either the $^1A_2$, ^1E_a or ^1E_b states is allowed

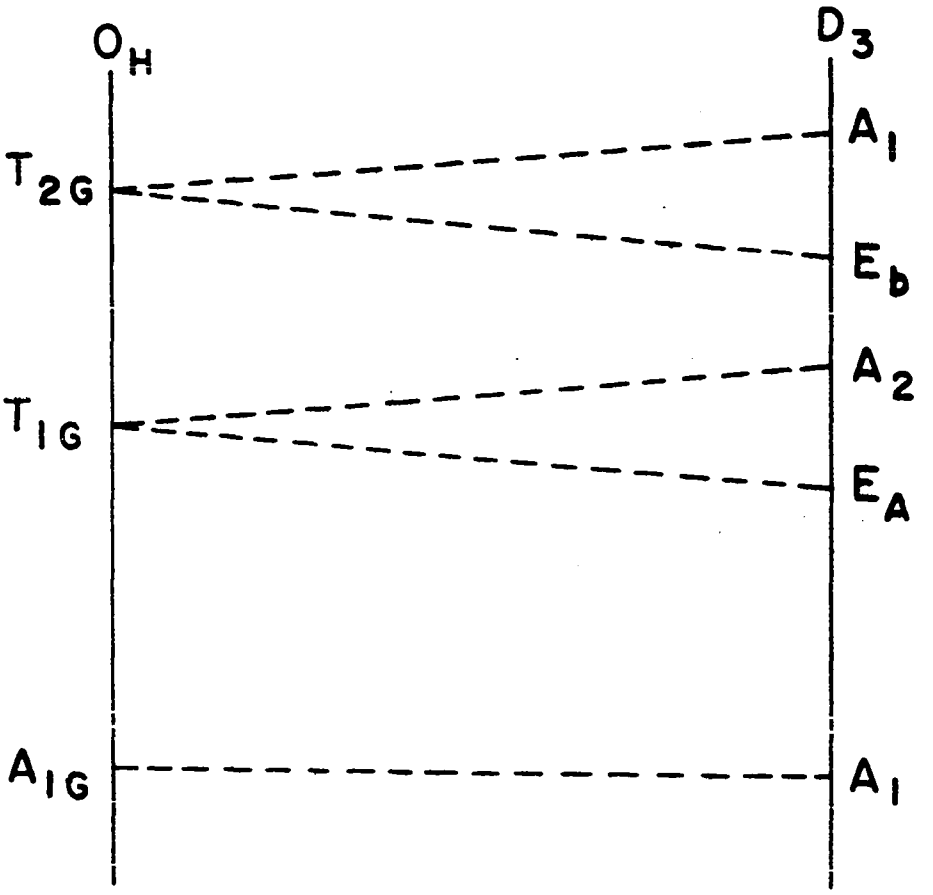

Figure 5. Reduction from O_h to the lower D_3 symmetry for the energy states

in both magnetic and electric dipole radiation fields and they should have a finite Cotton effect, whereas the $^1A_1$ transition is forbidden, and should have zero effect.

If circularly polarized light is passed along the C_3 axis of the $[Co(en)_3]^{3+}$ ion, in the crystalline structure $2[Co(en)_3](Cl_3)\cdot NaCl\cdot 6H_2O$, only those transitions with E symmetry are allowed (9). By comparing the crystal and solution spectra (Figure 6) of the complex it is clear that:

a) $^1A_1 \rightarrow {}^1E_a$ is at lower energy than $^1A_1 \rightarrow {}^1A_2$

b) $^1A_1 \rightarrow {}^1E_b$ gives a positive Cotton effect.

The above results have led to a spectroscopic criterion for inferring absolute configurations; (+)5890A-$[Co(en)_3]^{3+}$ has the Λ-configuration (Figure 7) from X-ray analysis (10) and $^1A_1 \rightarrow {}^1E_a$ in this complex gives a positive Cotton effect. Consequently, if an E_a transition has a positive Cotton effect for the dihedral d^3 or d^6 complexes it is assumed to have the Λ absolute configuration. This criterion applies to all cases where the configurations have been confirmed.

D. History

1. Thermal racemization

LeMay and Bailar (11) reported the solid-state racemization of l-cis-$[Cr(en)_2Cl_2]Cl\cdot H_2O$. They studied both the dehydration and racemization processes of this complex. They concluded that the racemization can be interpreted in terms of an aquation-anation pathway. The samples were

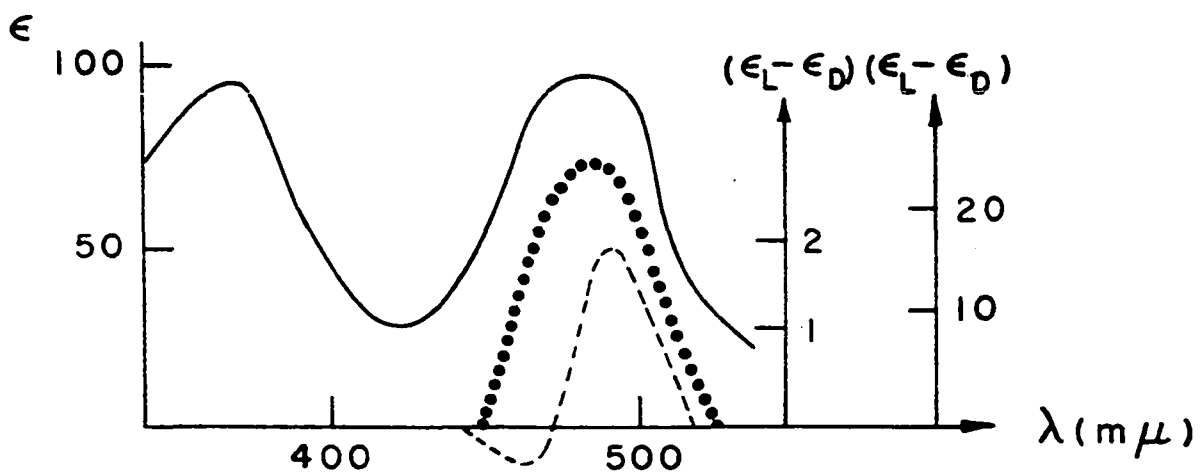

Figure 6. Splitting of low energy band for D-$[Co(en)_3]^{3+}$: (_____) absorption; (-----) circular dichroism in solution (inner scale); (.....) circular dichroism in oriented crystal (outer scale)

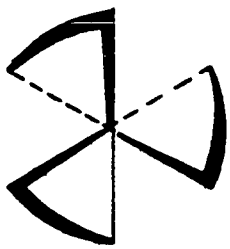

(a)

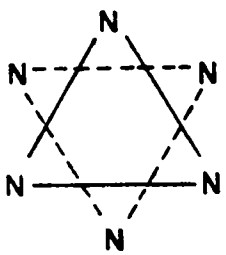

(b)

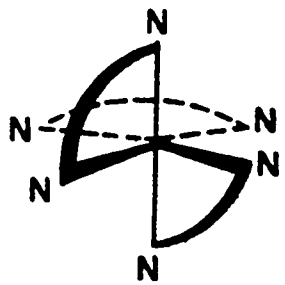

(c)

Figure 7. The absolute configuration of D-$[Co(en)_3]^{3+}$:
(a) Arrangement of chelate rings
(b) Arrangement of nitrogen atoms viewed about the threefold axis
(c) Viewed along the twofold axis

heated to the following temperatures: 120, 138, 140, 160 and 180°C, at a rate of 2-5°/min., a thermorgravimetric instrument was used. It was noted that very little, if any, racemization occurred after the initial loss of one mole of water/mole of complex present. At each temperature they reported the mass loss was more rapid than racemization. The analogous cobalt compound, $[Co(en)_2 Cl_2]Cl \cdot H_2O$ was found to undergo solid-state racemization, also with the loss of a mole of water/mole of complex. But after the mass loss had ended the compound continued to racemize. Ultraviolet spectra and elemental analysis verified that no conversion to the trans-isomer or decomposition had taken place. When D-$[Co(en)_3](I)_3 \cdot H_2O$ was heated to 110°C at a rate of 1°/min. one mole of water was evolved/mole of complex. After heating to 140-143°C for 18-20 hours the specific rotation was half the original value. After heating at 170°C for 14-16 hours the complex was completely racemized. They concluded by stating that one should consider the possibility of aquation-anation pathways for hydrated complexes but this need not be the only method.

Kutal and Bailar (12) have studied the solid-state racemization of (+)-$[Co(en)_3](X)_3 \cdot nH_2O$, (where X = Cl^-, Br^-, I^-, NCS^- and n = 0,1). The results of their investigation indicated that the hydrated iodide and bromide complexes racemize considerably faster than their anhydrous analogs.

They attributed the effect to physical modifications of the lattice during the dehydration rather than the displacement of an ethylenediamine molecule with a water molecule. The anhydrous complexes were found to racemize in the following order: $I^- > Br^- > NCS^- > Cl^-$. This sequence of anions, for the racemization process, follows the expected order for the decrease in hydrogen bonding in the complexes. The actual mechanism for the racemization was attributed to a twist mechanism, which again would be dependent upon the degree of hydrogen bonding in the complexes. Most of the kinetic studies reported were studied at a temperature of 127°C. No rate constants were reported for the solid-state racemization studies. The reasons given for not including any rate expressions was that they didn't have a suitable hypothesis for the mechanism of the reaction. An activation energy of 61 ± 10 Kcal-mole^{-1} was reported for the solution racemization of the $[Co(en)_3](I)_3$ complex.

Kutal (13) reported that $[Co(en)_3](I)_3 \cdot H_2O$ loses 96% of its water of hydration between 60-90°C, from thermogravimetric analyses. The analogous bromide complex lost its water of hydration in a single step between 70-100°C. The chloride complex lost its water of hydration in a single step between 101-123°C. He also reported that the experimental temperatures were dependent on the particle size of the samples, (i.e. the finer samples would lose water

at a lower temperature). This same particle size dependence was noted in the racemization studies.

2. X-ray crystal structure

The crystal structure of the tris(ethylenediamine)-cobalt(III) ion has been reported by several investigators, the results of their work is presented below.

The structure of tris(ethylenediamine)cobalt(III)-chloride monohydrate, completed by Iwata, Nakatzu and Saito (14), belongs to the tetragonal crystal class having $\underline{a} = \underline{b} = 9.682 \pm 0.002$A, $\underline{c} = 16.287 \pm 0.002$A; density (measured) = 1.585 g-cm^{-3}; Z = 4; volume = 1527A^3 and space group $\underline{P}4_3 2_1 2$.

The structure of tris(ethylenediamine)cobalt(III)bromide monohydrate, completed by Nakatsu (15), belongs to the tetragonal crystal class having $\underline{a} = \underline{b} = 9.95 \pm 0.03$A, $\underline{c} = 16.73 \pm 0.05$A; density (measured) = 1.971 g-cm^{-3}; Z = 4; volume = 1656A^3 and space group $\underline{P}4_1 2_1 2$ or $\underline{P}4_3 2_1 2$.

A preliminary study, by Kutal and Bailar (12), of tris(ethylenediamine)cobalt(III)iodide monohydrate indicated the crystal belonged to the orthorhombic crystal class with $\underline{a}$ = 8.44A, $\underline{b}$ = 18.95A and $\underline{c}$ = 11.28A; density (measured) = 2.32 g-cm^{-3}; Z = 4; volume = 1844A^3 and space group $\underline{P}2_1 2_1 2_1$.

3. Ultraviolet photolysis

The energy gained by a molecule when it absorbs a light quantum is given by Bohr's equation:

$$\Delta E = h\nu$$

where h is Planck's constant and ν is the frequency (sec^{-1}) of the radiation. The efficiency of a photochemical process, i.e. the quantum yield (Φ) is defined as:

$$\Phi = \frac{\text{\# of molecules undergoing that process}}{\text{\# of photons absorbed by the reactant}} .$$

When the products of the primary chemical process are radicals or other unstable compounds, they may undergo secondary thermal reactions. In these cases, the experimentally measured quantum yield may be either higher (owing to chain reactions) or lower (owing to a cage effect or other back reactions) than the primary yield.

Photoactivation is the first process involved in a photochemical sequence:

$$A + h\nu \rightarrow A^*$$

The electronically excited molecules so obtained must lose their excess energy in order to place themselves in equilibrium with their surrounding environment. This deactivation of the excited molecule is achieved through either chemical or physical processes. The physical deactivating processes may be subdivided into radiative and non-radiative; the latter ones include first order processes (unimolecular radiationless transitions) and second order processes (bimolecular quenchings):

$A^* \rightarrow A + h\nu$ radiative deactivation

$A^* \rightarrow A +$ heat radiationless deactivation

$A^* + Q \rightarrow A + Q^*$ bimolecular quenching.

A radiationless transition is a unimolecular process in which the energy difference between the initial and final states eventually appears as heat in the surrounding medium. This process essentially consists of an isoenergetic conversion of the electronic energy in an upper state into vibrational energy in a lower state of the same molecule, followed by the dispersion of the excess vibrational energy of the lower state into the surrounding medium.

Bimolecular quenching is an intermolecular transfer of energy from a donor (D) to an acceptor (A) molecule:

$$D^* + A \rightarrow D + A^*.$$

The energy transfer between the donor and acceptor may occur by various mechanisms: one being the case of emission from D* and re-absorption by A, and another, the intramolecular transfer which occurs when D* and A associate to give a metastable complex that dissociates into D and A*.

All studies of the photoreduction of cobalt(III) complexes have been carried out in acidic solution; the long lifetimes of cobalt(II) ammines in basic solutions lead to complicated reactions because of the easy reoxidation of amine-coordinated cobalt(II) to the corresponding cobalt(III) complex. Precipitation of cobalt oxides is another complicating factor under basic conditions.

The photochemical behavior of cobalt(III) complexes in aqueous solution is characterized by the simultaneous

photoaquation and photoredox decomposition reactions. From a kinetic point of view, most of the cobalt(III) complexes are rather inert. When considering redox reactions it should be noted that in aqueous solutions containing no complexing agents cobalt(III) is very unstable with respect to the reduction to cobalt(II):

$$[Co(H_2O)_6]^{3+} + e^- \rightarrow [Co(H_2O)_6]^{2+} \quad E^o = 1.93 \text{ v (16)}.$$

The stability of cobalt(III) is greatly enhanced upon complexation with suitable ligands, as shown by the values of the redox potentials for the following reactions:

$$[Co(ox)_3]^{3-} + e^- \rightarrow [Co(ox)_3]^{4-} \quad E^o = 0.57 \text{ v (17)}$$

$$[Co(NH_3)_6]^{3+} + e^- \rightarrow [Co(NH_3)_6]^{2+} \quad E^o = 0.06 \text{ v (18)}$$

$$[Co(en)_3]^{3+} + e^- \rightarrow [Co(en)_3]^{2+} \quad E^o = -0.26 \text{ v (18)}.$$

It should be remembered that cobalt(II) is a labile d^7 system and thus its complexes undergo rapid dissociation in acid solution.

An investigation of the photochemical decomposition of the $[Co(en)_3]X_3$ complexes, in the solid state, ($X = F^-$, Cl^-, Br^- and I^-) was carried out by Klein, Moeller and Ward (19). They observed that radiation of wavelength 2537A was strongly reactive, while radiation of wavelength 3650A or longer did not cause any change in the complex. Polarographic analysis, spectrophotometric studies, magnetic susceptibility measurements, infrared spectra and mass spectrometer studies were performed in order to clarify the nature of the photolysis

products. The presence of cobalt(II) in the photolyzed solid compound showed that some oxidation-reduction process involving the central metal atom had to occur. Ammonia was the only gaseous product identified, and chemical analysis indicated that two molecules of ammonia were eliminated for each atom of cobalt reduced. The lack of evidence for Cl or Cl_2 and the presence of three chloride ions per cobalt(II) atom after photolysis of $[Co(en)_3](Cl)_3$ suggested that halide oxidation was not involved in the photolysis reaction. Quantitative analysis of the photolysis product indicated that it contained a 1:1 ratio of Co(III):Co(II). The irradiations were carried out for a 20 hour time period. The cobalt(II) was present as tetracoordinated anion, while the cobalt(III) was present as an unidentified yellow complex, different from the initial $[Co(en)_3](Cl)_3$. They concluded that irradiation probably caused the formation of a cobalt(III) structure linked by polyamine condensation products of ethylenediamine.

In the same paper Klein, et al. (19) also reported studies on the photochemical behavior of other cobalt amine complexes in the solid-state. On ultraviolet irradiation $[Co(pn)_3](Cl)_3$ (pn = 1,2-diaminopropane) was found to change its color from orange to green, with formation of cobalt(II) species. $[Co(NH_3)_6](Cl)_3$ exhibited a similar behavior. The order of photosensitivity, based on the amount of cobalt(II) formed, was $[Co(NH_3)_6](Cl)_3$ > $[Co(en)_3](Cl)_3$ > $[Co(pn)_3]$-

$(Cl)_3$. A more recent (20) investigation on $[Co(NH_3)_6](Cl)_3$ and $[Co(en)_3](Cl)_3$ showed that the amount of cobalt(II) formed increased with the duration of irradiation; kinetic calculations indicated a very complicated reaction mechanism was involved. In a later work Klein and Moller (21) reported the photolysis of aqueous solutions of $[Co(en)_3](Cl)_3$ gave different products than those in the solid state. They observed the production of a photosensitive cobalt(III)-ethylenediamine intermediate, ammonia, formaldehyde and cobalt(II). The quantitative analyses were not sufficiently precise to exclude the possibility of other photolysis products.

Taylor and Moeller (22) studied the ultraviolet photolysis of tris(propylenediamine)cobalt(III)chloride and tris(butylenediamine)cobalt(III)chloride in an acid medium. The major products of the decomposition reactions were cobalt(II) and ammonia. In addition for the propylenediamine complex, formaldehyde and ethylamine were formed and for the butylenediamine (bn) complex acetaldehyde and ethylamine were the additional products. (The butylenediamine complex was prepared from 2,3-diaminobutane).

Quantum yields for the reduction of cobalt(III) amines discussed are given below (at 2537A):

Compound	Quantum yield
$[Co(en)_3]^{3+}$	0.07
$[Co(pn)_3]^{3+}$	0.11
$[Co(bn)_3]^{3+}$	0.18

Spees and Adamson (23) reported no evidence for any photoracemization of $[Co(en)_3](Cl)_3$ using white light.

4. Gamma-ray radiolysis

On irradiation with Gamma-rays, from a ^{60}Co source in acid solution, the aquopentaammine and hexaammine complexes of cobalt(III) decompose to give cobalt(II) and nitrogen (24). The reaction is thought to involve an attack on the complexes by OH radicals, catalyzed by cobalt(II).

Neokladnova and Shagisultanova (25) have studied the gamma-ray radiolysis of $[Co(en)_3](Cl)_3$ in aqueous solutions. The solutions were subjected to radiation from a ^{60}Co source with the total dose varying from 2500 to 300,000 R. The solutions became alkaline and the precipitation of hydroxide occurred. The color of the solution turned red during the irradiation. They attribute this color change initially with aquation and subsequently with the formation of products of more extensive hydrolysis. It is known that the binuclear tetraethylenediamine complex has a ruby-red color. They give no quantitative or qualitative data concerning any products that were formed in the radiolysis process.

II. EXPERIMENTAL

A. Materials

1. Water

All water used in these experiments was tap distilled water which had been redistilled from alkaline permanganate.

2. Cobalt metal

Cobalt metal was obtained from the Analytical Department having a purity greater than 99 percent.

3. Alcohol

Absolute alcohol was obtained from the Warren and Douglas Company.

4. Other reagents

All other chemicals were reagent grade and were obtained from the Baker Chemical Company or Eastman Chemical Company.

B. Equipment

1. Spectropolarimeter and cells

The optical rotation spectra for this work were obtained with a Jasco Optical Rotatory Dispersion Recorder with Circular Dichroism attachment, Model ORD/UV-5. The cells used are made of fused quartz with a path length of one centimeter.

2. Spectrophotometer and cells

UV-Visible spectra were obtained using a Cary Model 14 spectrophotometer. The cells used were made of fused quartz with a one centimeter path length, obtained from the Beckman

Company.

3. IR spectrophotometer

Infrared spectra were obtained using a Beckman Model 12 IR spectrophotometer. Spectra were obtained with KBr discs.

4. NMR spectrometer

Nuclear magnetic resonance spectra were obtained on a Hitachi Perkin-Elmer R-20B High Resolution spectrometer or a Varian Model A-60 spectrometer.

5. Mass spectrometers

Low resolution mass spectra were recorded on a laboratory-built mass spectrometer (26).

High resolution mass spectra were obtained using the MS902 manufactured by AEI.

6. Thermogravimetric analyses

TGA curves were obtained using a Dupont 950 Thermogravometric Analyzer with a constant flow of dry nitrogen.

7. X-ray crystal structure apparatus

Precession photographs were obtained on Kodak Medical X-ray film using a Nonius precession camera. Data were collected using Mo K_{α} (0.7107A) X-rays. A Hilger-Watts four-circle diffractometer equipped with scintillation counter and using Zr-filtered Mo K_{α} (0.7107A) radiation was used in data collection.

8. X-ray racemization and sample holder

Mo radiation was used in the irradiation studies. A General Electric Model VER225 generator, set at 50 kilovolts and 20 ma was used as the power source. Fine powdered samples were pressed into a 0.5 in. diameter x 1/8 in. aluminum disc, held 1 in. from the X-ray tube and insulated on all sides with bakelite. The sample discs were enclosed in brass and lead shielding.

9. Gamma-ray source and sample holder

Fine powdered samples were placed in 1 in. diameter x 2.5 in. long polyethylene vials. The vials were lowered down a water tight aluminum pipe. The gamma-rays were produced by the spent fuel elements used in the Ames Laboratory Research Reactor.

10. UV-photolysis

The Rayonet Photochemical Reactor, manufactured by the Southern N. E. Ultraviolet Company, was used to irradiate the samples. Samples were irradiated with 2537A wavelength light in Vycor tubes, 9 mm in diameter and 12 in. long.

11. Sand bath and sample tubes

An Arthur A. Thomas TECAM sand bath was used in the thermal racemization studies. Sample tubes were made of Pyrex glass, 8 mm in diameter and 8 in. long.

12. TLD counter and chips

A TLD Reader Model TLR-5, Eberline Instrument Corporation, was used to count the LiF chips. The LiF (TLD-100) chips have dimensions 1/8 x 1/8 x 1/32 inches.

C. Preparations

1. Preparation and resolution of tris(ethylenediamine)-cobalt(III) ion (27)

$$4\ Co^{2+} + 12\ en + 4\ H^{+} + O_2 \rightarrow D,L\text{-}[Co(en)_3]^{3+} + 2\ H_2O$$

A 500 ml filter flask was fitted with a rubber stopper carrying an open glass tube extending to the bottom of the flask, and 20.4 ml of 88.6, (w/v) ethylenediamine (0.3 mole) was added. (The exact composition of the ethylenediamine was determined by dilution of a known volume with water and titration with standard acid, using methyl orange as the indicator). This solution was diluted with 50 ml water; the mixture was cooled in ice and 10 ml concentrated HCl added, (an equivalent amount of weaker or stronger acid could be used). Cobalt(II) sulfate heptahydrate (28.1 g, 0.1 mole), dissolved in 50 ml cold water was then added and finally activated charcoal (4 g). A rapid current of air was bubbled through the solution for 4 hrs. At the end of this time the pH of the mixture was adjusted by the addition of a few drops of either dilute HCl or ethylenediamine into a range 7.0-7.5. The mixture was then heated in an evaporating dish on a steam bath for 10-15 minutes to complete the reaction, it was

cooled and the charcoal filtered off. The charcoal was washed with 20 ml of water. Barium-D-tartrate (28.5 g, 0.1 mole) was added to the mixture and heated on the steam bath with good mechanical stirring for about 30 minutes. (Barium-D-tartrate was prepared by mixing solutions of barium chloride two-hydrate (24.4 g, 0.1 mole) and D-tartaric acid (15 g, 0.1 mole) at 90°C, cooling and then neutralizing with ethylenediamine until slightly basic. The crystals were separated by filtration and washed with warm water).

The barium sulfate, which precipitated initially, was filtered and washed with a little hot water and the red-orange filtrate was evaporated to a volume of 60 ml. Crystallization of the D-$[Co(en)_3]Cl$-D-tartrate-5-hydrate ensues on cooling and is completed by allowing the mixture to stand overnight. The crystals were filtered and the filtrate reserved for the isolation of the L isomer. The crystals were washed with 40% ethanol-water and recrystallized by dissolving in 30 ml of hot water followed by cooling to room temperature and then in ice. After filtration the crystals were washed with 40% ethanol-water, then with absolute alcohol, and air dried. Literature (27) $[\alpha]5890A$ = + 102°; found $[\alpha]5890A$ = + 102°.

2. <u>Preparation of D-tris(ethylenediamine)cobalt(III) bromide (28)</u>

To about 5 g of D-[$Co(en)_3$]Cl-D-tartrate-5-hydrate, which had been triturated, was added 10 ml warm concentrated hydrobromic acid (31). The resulting solution was allowed to stand for several hours. Dark red crystals, needles or tablets, of the acid crystals formed. These were recrystallized in hot water and air dried. Literature (28) $[\alpha]5890A = + 117°$; found $[\alpha]5890A = + 117°$.

3. Preparation of D-tris(ethylenediamine)cobalt(III) chloride (28)

$$D\text{-}[Co(en)_3]Br_3 + 3\ AgCl \rightarrow D\text{-}[Co(en)_3]Cl_3 + 3\ AgBr$$

The chloride complex was prepared from the bromide complex through the exchange with silver chloride. To an aqueous solution of 3 g of the bromide was added an excess of freshly precipitated silver chloride. The mixture was vigorously shaken for several minutes and filtered. The residue was washed with several portions of water, the filtrate was concentrated using a stream of dry air. To accelerate the crystallization a few ml of alcohol was added to the filtrate. Literature (28) $[\alpha]5890A = + 152°$; found $[\alpha]5890A = + 151°$.

4. Preparation of D-tris(ethylenediamine)cobalt(III) nitrate (28)

$$D\text{-}[Co(en)_3]Br_3 + 3\ AgNO_3 \rightarrow 3\ AgBr + D\text{-}[Co(en)_3](NO_3)_3$$

A hot solution of silver nitrate (3 mole) was added to D-[$Co(en)_3$]Br_3 (1 mole) dissolved in a minimum amount of

water. The mixture was allowed to cool to room temperature. The yellow precipitate of silver bromide was filtered and washed with a little water. The filtrate was condensed and cooled. The orange-yellow crystals of the nitrate were filtered and air dried. Recrystallization was from water. Literature (28) $[\alpha]5890A = +132°$; found $[\alpha]5890A = +130°$.

5. Preparation of acetamidine (29)

$$CH_3C(:NH)NH_2 \cdot HCl + NaOH \rightarrow CH_3C(:NH)NH_2 + NaCl + H_2O$$

By treating a cooled saturated solution of acetamidine hydrochloride with an excess of cold, almost saturated caustic soda, a colorless oil was obtained. After being dried over anhydrous calcium sulfate it can be kept for periods of days at -40°C, as a glassy solid without appreciable decomposition. The NMR spectrum, in D-water, has for the methyl protons a single peak at 2.25 ± .05 ppm. The hydrochloride salt, in D_6-DMSO, has the methyl singlet peak at 2.25 ± .05 ppm and two broad N-H singlets at 8.76 ± .05 and 9.31 ± .05 ppm. When NaOH was added to the solution the two N-H singlets coalesced into one broad peak at 8.5 ± .1 ppm. The methyl proton peak did not change. Sodium-2,2-dimethyl-2-silapentane-5-sulphonate was used as standard in all spectra.

D. Analysis and Results

1. Thermogravimetric analyses of tris(ethylenediamine)-cobalt(III) complexes

The thermal gravimetric analyses of the various complexes indicated that there are several points of inflection in the curves but very few distinct plateaus, this made identification of exact mass losses difficult.

The TGA curves for D-$[Co(en)_3]X_3$ (where X = Cl^-, Br^-, I^- and NO_3^-) were studied. In Table 1 is given the results of the TGA experiments for the various complexes which had not been irradiated.

The TGA curve (Figure 8) for the chloride salt indicates there is one water of hydration present. Between 25-245°C the sample loses its one water of hydration in several distinct steps. This could be due to the fast heating rate. Between 245-300°C 1.5 ethylenediamine molecules were lost, this corresponded to a total mass loss of 27.6%. Between 300-405°C an additional 1.5 ethylenediamine molecules were lost. Between 405-605°C a total mass loss of 76.5% was recorded, this corresponded to the additional loss of two chlorides. The last chloride came off in the range 615-910°C, total mass loss 83.8%. Cobalt metal corresponds to 16.3% of the complex. The sample was heated at a rate of 10°/min.

The TGA curve (Figure 8) for the bromide complex indicates there were no waters of hydration present. At about 265° the compound began to lose mass until a mass loss of 51.0% resulted. This corresponded to a loss of three

Table 1. Thermogravimetric results for $[Co(en)_3]X_3$. Heating rate = 10°/min

Temperature (°C)	Total % Mass Loss	Species lost	Theoretical % Mass Loss
		X = Chloride•H_2O	
25-245	5.0	H_2O	5.0
245-300	27.6	H_2O + 1.5 en[1]	29.7
300-405	50.1	H_2O + 3 en	54.7
405-615	76.5	H_2O + 3 en + Cl_2	74.2
615-910	83.8	H_2O + 3 en + 3 Cl	84.5
		X = Bromide	
25-258	0.0		
258-510	51.0	3 en + Br	54.3
510-860	88.8	3 en + 3 Br	87.7
		X = Iodide	
25-260	0.0		
260-400	28.4	3 en	29.1
400-460	50.0	3 en + I	49.5
460-960	90.2	3 en + 3 I	90.5
		X = Nitrate	
25-255	0.0		
255-271	13.2	detonates	

[1]en = ethylenediamine

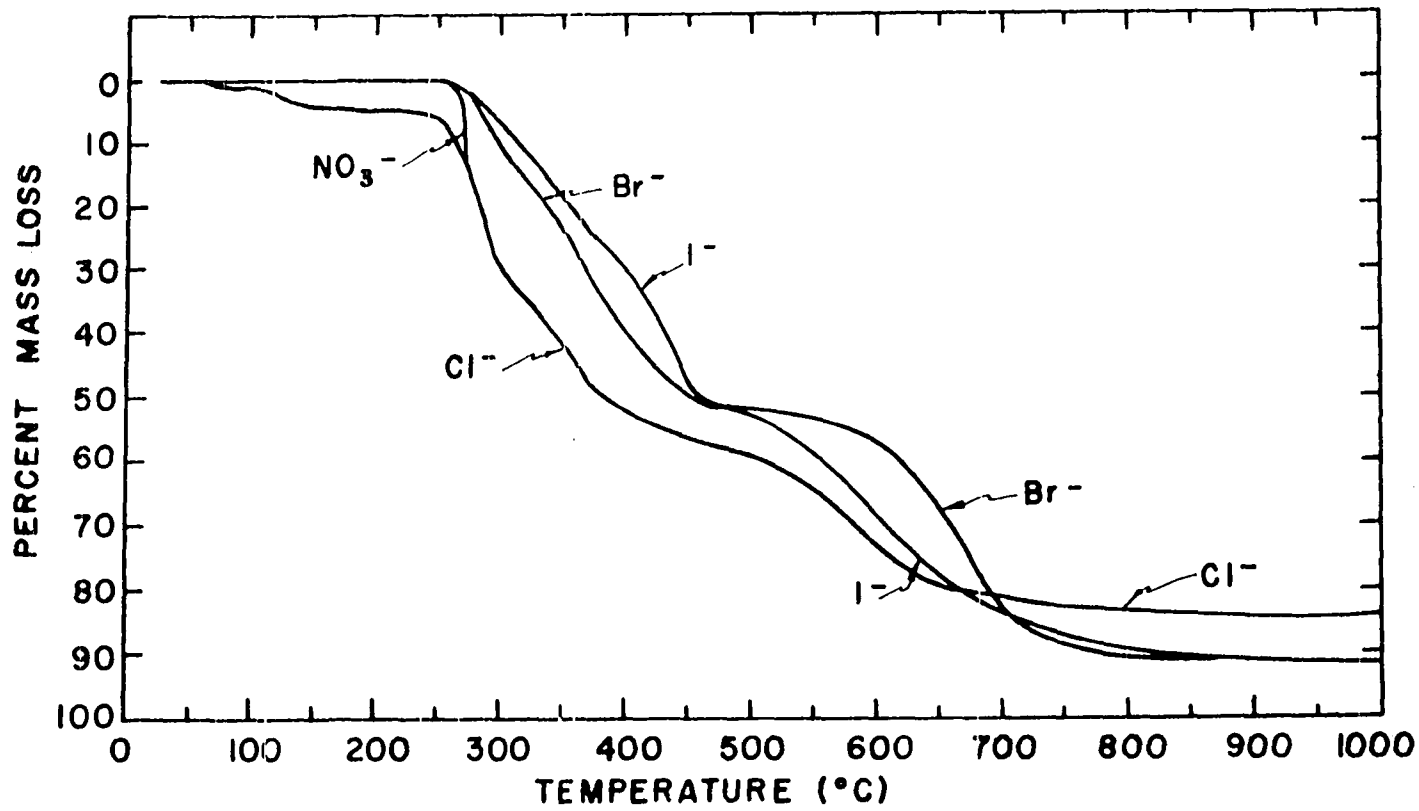

Figure 8. Thermogravimetric curves for $[Co(en)_3]X_3$ (where X = Cl^-, Br^-, I^- and NO_3^-. Heating rate = 10°/min

ethylenediamines and one bromide. At about 500° another mass loss began corresponding to the loss of two bromides, with a total mass loss of 88.8%. The plateau at 1000° corresponded to cobalt metal. Cobalt metal corresponds to 12.3% of the complex. The sample was heated at a rate of 10°/min.

The TGA curve (Figure 8) for the iodide complex indicates there are no waters of hydration present. At about 250° the compound began to lose mass until a mass loss of 28.4% resulted. This corresponded to a loss of three ethylenediamines. At about 390° another mass loss began corresponding to the loss of one iodide, with a total mass loss of 50.0%. At 460° began another mass loss, this appears to be a loss of two iodides. The plateau at 1000° corresponded to cobalt metal. Cobalt metal corresponds to 9.6% of the complex. The sample was heated at a rate of 10°/min.

The TGA curve (Figure 8) for the nitrate complex indicates there are no waters of hydration present. At about 270° (mass loss 13.2%) the sample detonated; the heating rate was 10°/min. In Table 2 is given the results of the TGA experiments for the irradiated nitrate complexes with heating rate equal to 10°/min.

Other samples of the nitrate complex were heated to 200°, at a rate of 10°/min., and then at a rate of 0.5°/min. between 200-250°. At 242° the non-irradiated complex detonated. Before detonating the mass loss was 30.7%.

Table 2. Thermogravimetric results for $[Co(en)_3](NO_3)_3$. Heating rate = 10°/min

Temperature (°C)	Type of Radiation	Total % Mass Loss	Deton. Temp.	Total Exposure (MR)
25-255		0.0		
255-271		13.2	271	0
25-50		0.0		
50-241	X-rays	24.5	241	61
25-50		0.0		
50-239	X-rays	23.9	239	66
25-180		0.0		
180-265	Gamma-rays	16.7	268	54
25-50		0.0		
50-265	Gamma-rays	18.7	265	104
25-50		0.0		
50-260	Gamma-rays	18.3	260	147
25-50		0.0		
50-258	Gamma-rays	18.5	258	185
25-40		0.0		
40-255	Gamma-rays	18.2	255	217

Slower heating rates were not attempted. Figures 9 and 10 show some of the TGA curves for the irradiated nitrate complex. In Table 4 is given the results of the TGA experiments, for the irradiated nitrate compounds, with heating rate equal to 0.5°/min. between 200-250°C.

2. Cobalt metal standard (30)

0.23615 g of high purity cobalt metal was dissolved in concentrated HCl. This was then diluted with water to one liter giving a cobalt(II) concentration of 0.23615 mg/ml. Various aliquots were taken to which was added a total concentration of 5% ammonium thiocyanate, and acetone to correspond to 60% of the total volume. The visible absorption spectrum was run and at 6230A the absorption noted. In Table 3 is listed the concentrations used and the absorbances measured for $[Co(SCN)_4]^{2-}$, Figure 11 is a plot of the data.

Table 3. Data used for the Absorbance versus Concentration plot of $[Co(SCN)_4]^{2-}$

mg Co / 10 ml Solution	Absorbance Measured
0.1134	0.248
0.2247	0.649
0.3401	1.038
0.3778	1.196
0.4723	1.590

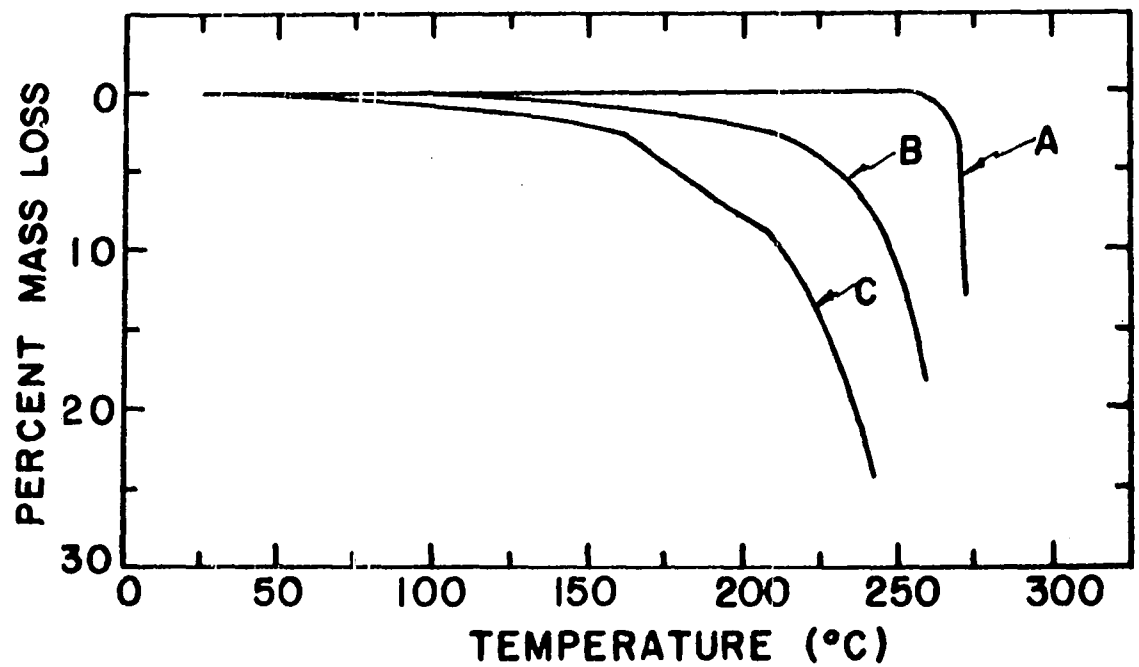

Figure 9. Thermogravimetric curves for $[Co(en)_3](NO_3)_3$.
Heating rate = 10°/min
(a) Non-irradiated complex
(b) Irradiated with gamma-rays, total exposure 147 MR
(c) Exposed to X-rays, total exposure 66.4 MR

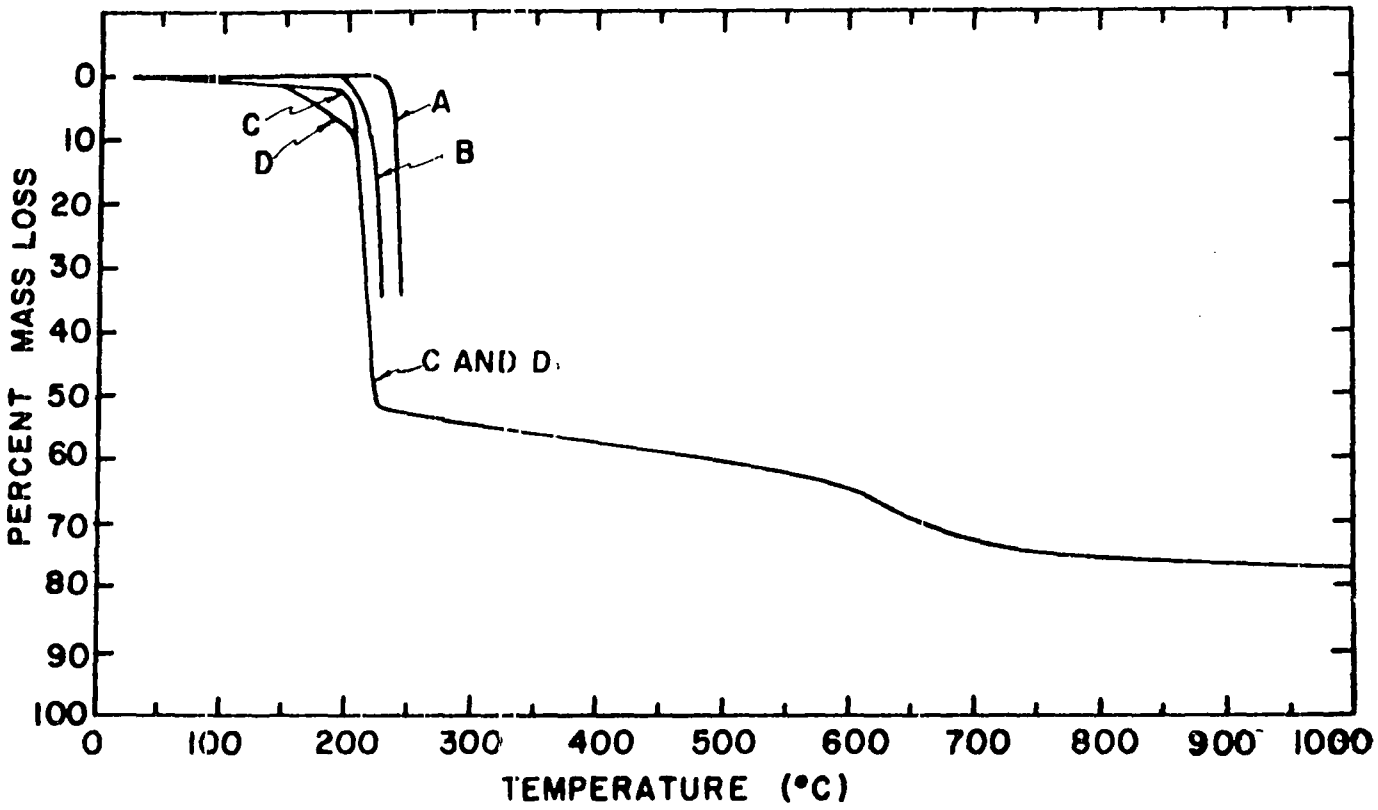

Figure 10. Thermogravometric curves for $[Co(en)_3](NO_3)_3$. Heating rate = 10°/min. Between 200-250° heating rate = 0.5°/min
(a) Non-irradiated complex
(b) Irradiated with gamma-rays, total exposure 54 MR
(c) Irradiated with gamma-rays, total exposure 147 MR
(d) Irradiated with X-rays, total exposure 66.4 MR

Table 4. Thermogravimetric results for $[Co(en)_3](NO_3)_3$. Heating rate = 10°/min, except between 200-250°C, where heating rate = 0.5°/min

Temp. (°C)	Total % Mass Loss	Species Lost	Theor. % Mass Loss	Total Exposure (MR)
25-225	0.0			
225-243	30.7	2 en[1]	28.2	0
243		detonates		
25-195	0.0			
195-228	32.4	2 en + NH_3	32.2	
228		detonates		54[2]
25-190	0.0			
190-230	53.5	3 en + NO_2	53.2	
230-600	67.5	3 en + NO_2 + 2 NO	67.3	
600-1000	77.4	3 en + NO_2 + 2 NO + 3/2 O_2	78.6	104[2]
25-50	0.0			
50-195	7.2	0.5 en		
195-230	51.2	3 en + NO_2	53.2	
230-605	67.5	3 en + NO_2 + 2 NO	67.3	
605-1000	76.5	3 en + NO_2 + 2 NO + 3/2 O_2	78.6	
1000	80.9	3 en + NO_2 + 2 NO + 2 O_2	82.4	66[3]

[1]en = ethylenediamine
[2]Exposed to gamma-rays
[3]Exposed to X-rays

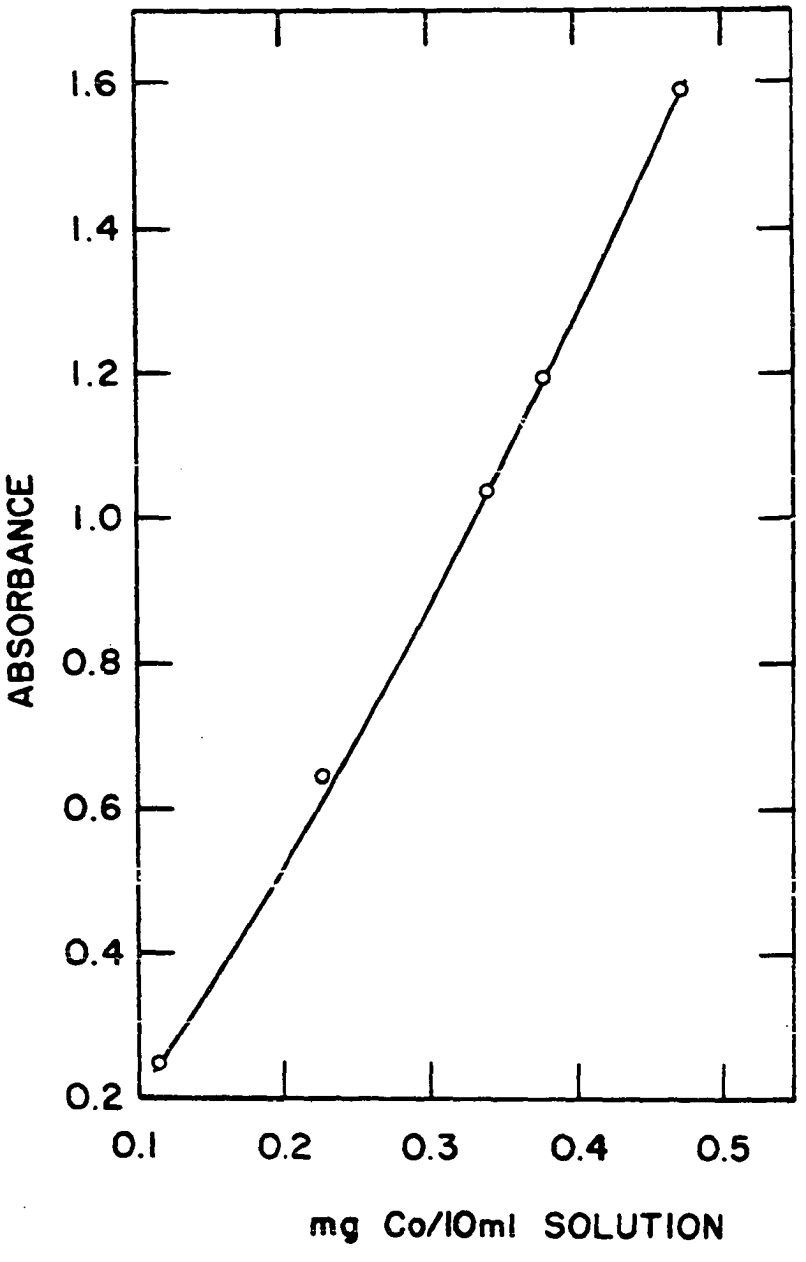

Figure 11. Absorbance as a function of concentration for $[Co(SCN)_4]^{2-}$

3. Analysis for cobalt(II) and cobalt(III) in irradiated $[Co(en)_3](NO_3)_3$ (30)

To about 0.02 g of the irradiated nitrate complex was added 1 ml of water and 3 drops of concentrated HCl. After the sample dissolved, 0.25 g ammonium thiocyanate was added and 1 ml water. The solution was diluted to 5 ml with acetone. The visible absorption spectrum of the $[Co(SCN)_4]^{2-}$ complex was recorded (Figure 12). The sample was washed into Vycor tubes (10 ml total volume) and photolyzed (31) for 8 hours at 2537Å. After this time 1 g ammonium thiocyanate was added and the solution diluted to 25 ml with a 60:40 acetone-water mixture. The visible absorption spectrum was then scanned. For the non-irradiated complex the amount of cobalt present was 14.1 ± .1% which compares favorably with the theoretical value of 13.9%. The results of the analyses, for the irradiated samples, are given in Table 5.

E. Calibration of Radiation Sources and Results

1. Units

The Roentgen (R) will be used as the measuring criteria in this work. A Roentgen is an exposure of X-radiation or gamma-radiation required to produce in air one electrostatic unit of charge of either sign per 0.001293 g of air at standard temperature and pressure (32). The Roentgen is a measure of the ability of a photon beam to produce ionization in

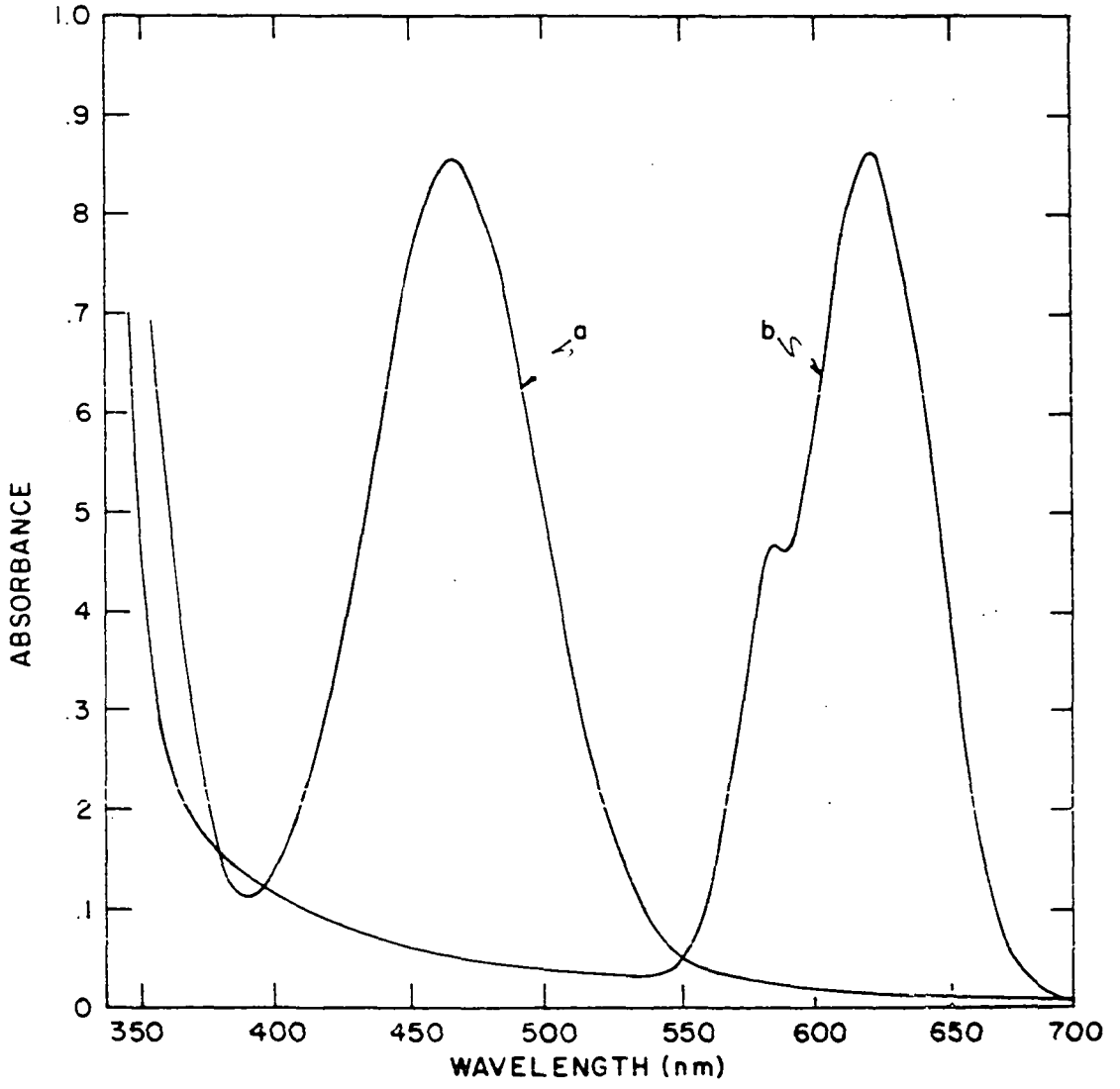

Figure 12. Visible absorption spectrum before and after UV-photolysis
(a) Before__$[Co(en)_3](NO_3)_3$
(b) After__$[Co(SCN)_4]^{2-}$

Table 5. Formation of cobalt(II) in irradiated samples of L-[$Co(en)_3$]$(NO_3)_3$

Sample	mg Co^{2+} (initial)	mg Co (total)	% Co	Mean (%)	Exposure (MR)
1	0.070	3.34	3.00		
2	0.075	3.09	2.43	2.58 ± 0.37	54[1]
3	0.069	3.00	2.30		
1	0.116	2.84	4.08		
2	0.120	3.00	4.00	4.05 ± 0.04	104[1]
3	0.122	3.00	4.07		
1	0.179	3.45	5.19		
2	0.163	2.94	5.54	5.41 ± 0.19	147[1]
3	0.163	2.96	5.51		
1	0.189	3.06	6.18		
2	0.206	3.23	6.38	6.25 ± 0.11	185[1]
3	0.195	3.15	6.19		
1	0.255	3.16	8.07		
2	0.243	2.85	8.53	8.19 ± 0.30	217[1]
3	0.240	3.01	7.97		
1	0.220	2.53	8.69		
2	0.245	2.55	9.61	8.89 ± 0.65	61[2]
3	0.230	2.75	8.36		
1	0.258	2.50	10.32		
2	0.290	2.83	10.25	10.29 ± 0.04	66[2]
3	0.274	2.66	10.30		

[1]Exposed to gamma-rays
[2]Exposed to X-rays

air. The Roentgen can be used directly only in discussing the amount of ionization produced in a finite volume of air.

2. X-ray facility

Thermoluminescence dosimetry (33) using LiF (TLD-100) crystals, was used to calibrate the X-ray source. When a sample is bombarded by X-rays it absorbs energy and some of this energy is stored in metastable energy states. This energy can be released by heating the sample and by measuring the light given off. The light given off is measured by a photomultiplier tube in a commercial instrument. The measurement is then compared with known standard curves from which the experimental exposure can be determined. Four LiF chips were placed in the sample holder at one time. This covered most of the surface area seen by the samples. The results of the calibration indicate that the chips were exposed to 0.36 ± 0.04 MR/hr. (M = mega).

3. Gamma-ray facility

Fricke dosimetry (34), $FeSO_4$ in H_2SO_4, was used to calibrate the gamma-ray source. The method compares the optical density of the iron(III) ion concentration of an irradiated solution to a non-irradiated solution, at 3050A. The exposure rate (R) is given by the empirical relation:

$$R(R/hr) = 10^9(A\underline{s} - A\underline{b})/(\varepsilon \cdot Y \cdot t)$$

where ε is the molar extinction coefficient (2174 l-mole^{-1}-cm^{-1} at 23.7°C); Y is the iron(III) sulfate yield

(about 16 micromolar/1000 R over the range 4-4000 KR); t is in hours; A_s is the absorbance of the sample and A_b the absorbance of the blank. The calibration of the beam was performed once during the irradiation period. This calibration point was then used to adjust a known measured decay curve for the fuel element fission product gamma-ray. The calibration work was performed by the Reactor Division personnel. The data and results of these experiments are given in Table 6.

Table 6. Calibration of gamma-ray facility

Date	Rate (MR/hr.)	Total Exposure (MR)
May 23, 72	0.368	0
May 30, 72	0.318	54
June 6, 72	0.275	104
June 13, 72	0.238[1]	147
June 20, 72	0.208	185
June 27, 72	0.182	217

[1]Fricke calibration point

F. Procedures

1. Thermal racemization

Powdered samples of the various compounds were weighed on an analytical balance and then placed in glass tubes. In the tops of the glass tubes was placed a plug of glass wool, to prevent sand from entering the tubes. The sample tubes were then inserted into the sand bath, as quickly as possible. At appropriate time intervals a tube would be removed from the sand bath and immersed in a beaker of ice water. The sample was then dissolved in water and diluted to volume. The ORD and UV-Visible spectra were obtained. The specific rotation was calculated for each sample. The measured rotation corresponded to the difference between the peak at 5200A and the valley at 4680A.

2. X-ray racemization

Samples of the various compounds were triturated to a fine powder and then pressed into their respective sample discs. The discs were then mounted in the sample holder one inch from the exit of the X-ray beam. At appropriate time intervals the X-ray beam was shut off and the sample removed. The samples were then weighed, dissolved in water and diluted to volume. The spectra were recorded as in (1) above.

3. Gamma-ray racemization

Samples of the nitrate salt were placed in polyethylene tubing, heat sealed at both ends. These tubes were then placed in a polyethylene vial equipped with screw cap. The vial was placed in an aluminum holder which was then lowered down a water-tight aluminum pipe, located in the pool at the Ames Laboratory Research Reactor. At appropriate time intervals a sample was withdrawn and spectra recorded as in (1) above.

4. Mass spectra

After a sample of the nitrate salt had been irradiated with X-rays it was placed in a double chambered glass bulb. The chamber in which the sample was placed was equipped with a rubber septum covered with a layer of mercury. The entire bulb was evacuated, each chamber was then closed and one ml of water was injected through the rubber septum onto the sample. After the sample had dissolved, the stopcock separating the two chambers, was opened allowing any gases to expand into the second chamber. The sample chamber was then closed off and the bulb attached to the mass spectrometer for analysis.

5. Crystal structure of D-$[Co(en)_3](NO_3)_3$

For data collection, a crystal having approximate dimensions 0.07 x 0.07 x 0.08 mm along the a, b, c crystal axes, respectively, was mounted with the 0.08-mm axis along the

spindle axis. The final alignment of the crystal was then adjusted by rotation through a few degrees before commencing to collect data to eliminate the occurrence of multiple reflections. A right-handed coordinate system was used.

Data were collected at room temperature (22 ± 3°C) utilizing a Hilger-Watts four circle diffractometer equipped with scintillation counter and using Zr-filtered Mo K_α (λ = 0.7107Å) radiation. Within a two theta sphere of 60° all data in one octant was recorded using the stationary crystal-stationary counter technique with a take-off angle of 6°. Peak height data were converted to integrated intensities by the method of Alexander and Smith (35). Stationary crystal-stationary counter background counts of 5 sec. were taken at $\Theta = \Theta_{hkl} \pm (0.25 + 0.01\Theta_{hkl})$ and peak heights were measured for 10. sec. A total of 2647 reflections were measured in this way.

As a general check on electronic and crystal stability the intensities of three standard reflections (10,00, 060, 006) were remeasured periodically during the data collection period. These reflections did not change significantly and therefore no corrections were made.

The intensity data were corrected for Lorentz-polarization effects. The absorption coefficient, μ, is 10.4 cm^{-1}. The maximum and minimum transmission factors are 92.9% and 92.3%, respectively. These were calculated by using the

minimum and maximum path lengths. Because the transmission factors are large, no absorption corrections were made. Of the 2647 measured intensities, 1943 were found to be above background (i.e. greater than three times the standard error based on counting statistics) and, therefore, considered as observed. The standard errors in the intensities and the observed structure functions were calculated by the method of Williams and Rundle (36) and are given by

$$\sigma_I = [\ TC + BG + (.05TC)^2 + (.05BG)^2]^{1/2}$$

$$\sigma_F = (L_p)^{-1/2}[\ (I + \sigma_I)^{1/2} - I^{1/2}].$$

Where I was the measured intensity equal to TC - BG; TC was the total counts; BG was the background counts; and L_p was the Lorentz-polarization. The function for σ_F is based on the finite difference method. The unobserved reflections were not used in the solution and refinement of the derived structure.

The unit cell parameters at 22 ± 3°C are: $\underline{a}$ = 14.570 ± 0.017A, $\underline{b}$ = 12.607 ± 0.016A, and $\underline{c}$ = 8.756 ± 0.003A. These parameters and their standard deviations were obtained by centering the diffractometer on independent reflections whose maxima were determined by left-right, top-bottom beam splitting on a previously aligned Hilger-Watts four-circle diffractometer (Mo K_α radiation, λ = 0.7107A). A calculated density of 1.756 g/cm^3 for four molecules per unit cell

agrees reasonably well with the observed density of 1.773 g/cm^3 obtained by flotation techniques.

III. TREATMENT OF DATA

A. Thermal Racemization

The rate constant reported in this investigation, for the racemization process, which presumably is a first order process, was derived by the following:

For the reaction:

$$D \underset{\leftarrow}{\overset{k}{\rightarrow}} L$$

The rate is given by:

$$(d[D]/dt) = k[L] - k[D]$$

the brackets designate the fraction of the sample in the indicated form

and

$$[\alpha] = ([D] - [L])[\alpha_D]$$

$$[\alpha_o] = ([D_o] - [L_o])[\alpha_D]$$

$$[1] = [D] + [L]$$

therefore

$$(d[D]/dt) = \{k[1 - D] - k[D]\}[\alpha_D]$$

$$= \{k[1 - 2D]\}[\alpha_D]$$

integrating from t = 0 to t and from D_o to D

$$\ln\{[1 - 2D]/[1 - 2D_o]\} = -2kt$$

or

$$\ln\{[\alpha]/[\alpha_o]\} = -2kt$$

and

$$k = -1/(2t) \cdot \ln\{[\alpha]/[\alpha_o]\}$$

All racemization data were fitted by the least squares method. A computer program was used to facilitate data processing.

The results of the thermal racemization studies are listed in Table 7. Absorption spectra for the various complexes indicated that there was no decomposition taking place during the thermal heating. Figure 13 shows some typical racemization results for the various complexes. Figure 14 shows the results of the rate constants plotted against one over the absolute temperature.

B. Crystal Structure of D-$[Co(en)_3](NO_3)_3$

1. Precession photographs

Microscopic examination of the crystals revealed that they were either triangular prisms or needles with sharply defined faces. A needle crystal was selected for diffraction work. Preminiinary precession photographs exhibited mmm symmetry, as did the triangular prisms, indicating an orthorhombic space group. The conditions limiting the possible reflections were $h00$, extinct if $h = 2n + 1$; $0k0$, extinct if $k = 2n + 1$; and $00l$, extinct if $l = 2n + 1$. These conditions uniquely determine the space group $P2_12_12_1$.

2. Patterson and electron density maps

A three-dimensional Patterson synthesis was computed from the data and careful analysis revealed the position of the cobalt atom. A pseudo extinction of the type hkl, $h + l$

Table 7. Thermal racemization results for $[Co(en)_3]X_3$ complexes

Temperature (°C)	Number of Experiments	Rate Constant (min^{-1})	Half-life (min)
		X = Chloride•H_2O	
170	3	$(1.3 \pm .3) \times 10^{-3}$	530 ± 120
186	5	$(1.6 \pm .4) \times 10^{-2}$	44 ± 5
204	3	$(1.6 \pm .3) \times 10^{-2}$	44 ± 7
214	3	$(5.5 \pm .1) \times 10^{-2}$	13 ± 2
		$\Delta H = 29.7 \pm 4.5$ Kcal-mole^{-1}	
		X = Bromide	
140	1	$(8.0 \pm .1) \times 10^{-5}$	8500 ± 460
158	3	$(1.6 \pm .5) \times 10^{-4}$	4300 ± 1200
183	4	$(9.0 \pm .1) \times 10^{-3}$	77 ± 10
194	5	$(3.9 \pm .5) \times 10^{-3}$	180 ± 20
204	4	$(1.3 \pm .2) \times 10^{-2}$	53 ± 6
		$\Delta H = 33.2 \pm 3.6$ Kcal-mole^{-1}	
		X = Iodide	
140	1	$(2.5 \pm .1) \times 10^{-4}$	2700 ± 54
158	3	$(3.0 \pm .2) \times 10^{-3}$	230 ± 16
169	5	$(1.7 \pm .2) \times 10^{-3}$	410 ± 38
185	5	$(1.5 \pm .5) \times 10^{-2}$	48 ± 16
		$\Delta H = 29.1 \pm 4.6$ Kcal-mole^{-1}	
		X = Nitrate	
218	5	$(2.3 \pm .5) \times 10^{-4}$	3000 ± 640
224	3	$(6.0 \pm .1) \times 10^{-4}$	1200 ± 170
233	3	$(6.5 \pm .1) \times 10^{-3}$	110 ± 17
		$\Delta H = 108.9 \pm 5.8$ Kcal-mole^{-1}	

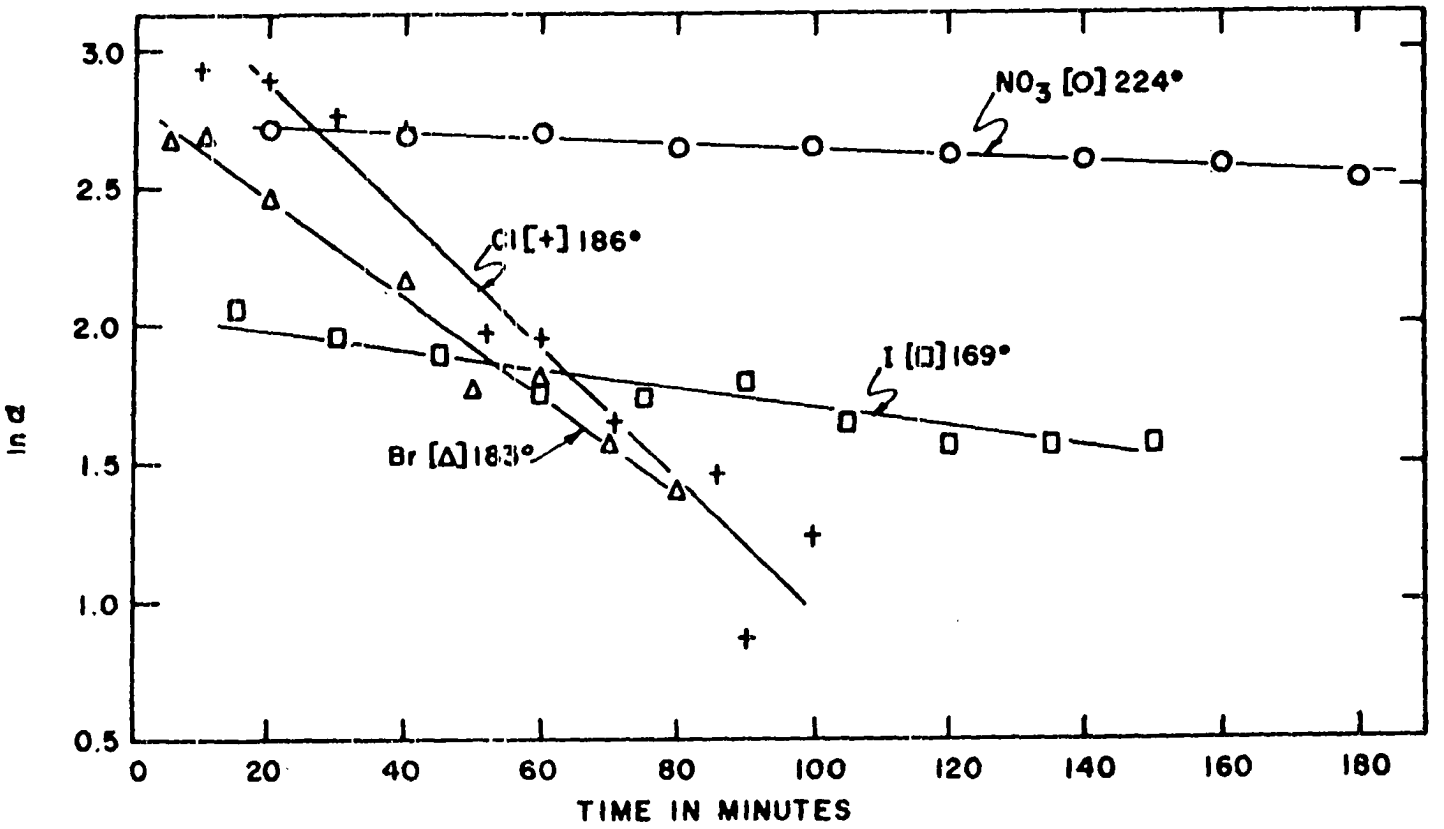

Figure 13. Racemization curves for the various salts of $[Co(en)_3]^{3+}$

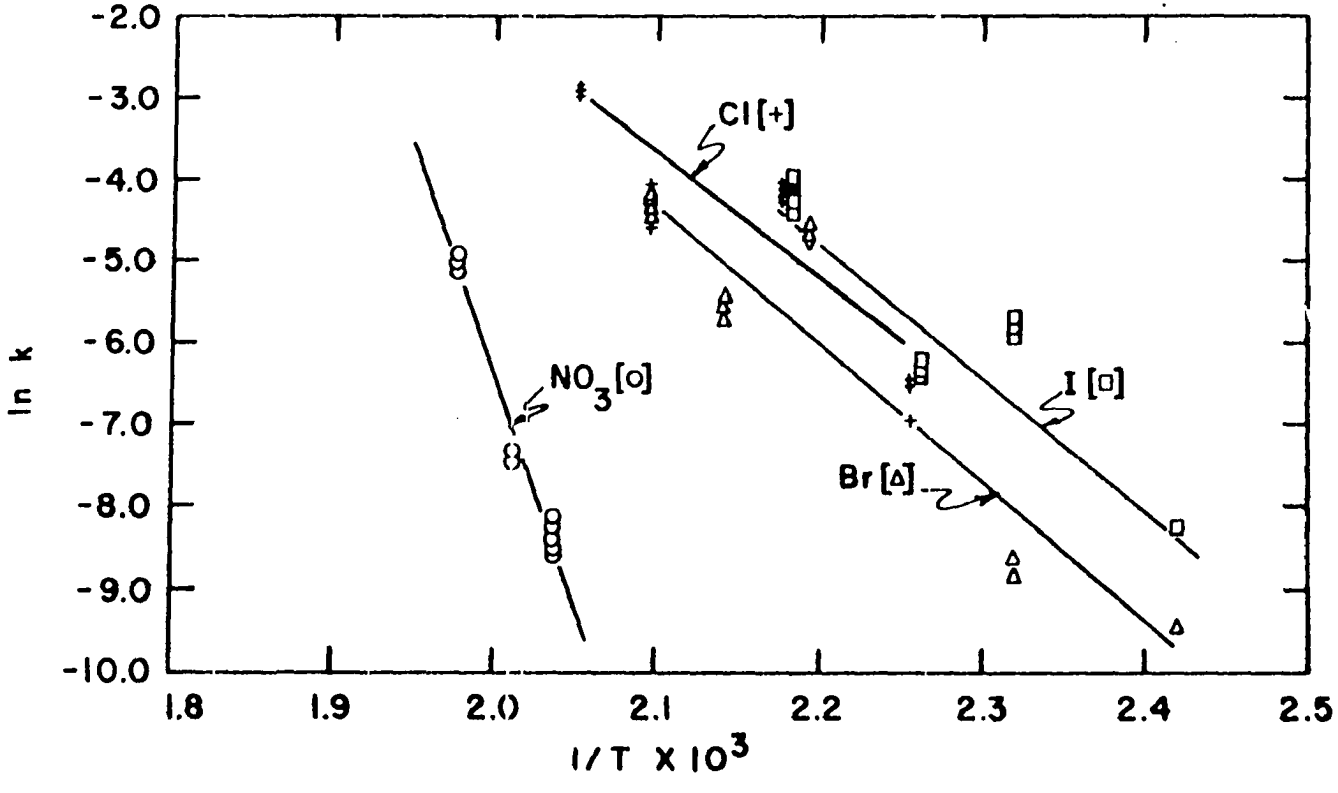

Figure 14. Temperature dependence for the specific rate constants of $[Co(en)_3]^{3+}$ salts

= 2n + 1 occurs and indicative of pseudo B centering. This was interpreted to mean that the cobalt atom was midway between the screw axes along x and at y = 1/4, z = 3/4. The cobalts' location caused a pseudo-twofold axis in the z direction in the electron density map. This pseudo-axis disappeared after careful placement of the other atoms. These positions were then refined by full matrix least-squares techniques with isotropic thermal parameters to a conventional discrepancy factor of $R = \Sigma ||F_o| - |F_c||/\Sigma|F_o| = 0.108$ and a weighted R factor of $\omega R = [\Sigma\omega (|F_o| - |F_c|)^2/-\Sigma\omega|F_o|^2]^{1/2} = 0.134$. The scattering factors were those of Doyle and Turner (37).

A difference electron density map at this stage showed that all the non-hydrogen atoms had been accounted for, but that some anisotropic motion was evident. The anisotropic refinement was carried out in two steps. First, the complex was varied and then the nitrates with the cobalt atom held common in both refinements. This was done because of the large number of variables in the total molecule. After a few cycles the final values of R and ωR of 0.085 and 0.101, respectively, were obtained. Modifications for the real and imaginary parts of the anomalous dispersion, taken from Cromer and Liberman (38), were now added. The final values of R and ωR of 0.084 and 0.100, respectively, were obtained. A final electron density difference map shows no peaks higher

than $0.5e/A^3$. A final statistical analysis of the F_o and F_c values as a function of the indices, the scattering angle and the magnitude of F_o showed no unusual trends and suggests that the relative weighting scheme used is a reasonable one.

In Table 8 are listed the final values of the positional parameters and in Table 9 the final values for the anisotropic temperature factors, along with their standard deviations as derived from the inverse matrix. In Table 10 are listed the values of F_o and F_c in electrons for the 1943 observed reflections. The values of F_o for the unobserved reflections in no case exceeded $3\sigma(F_o)$. In Table 11 are listed the calculated hydrogen positions for the carbon and nitrogen atoms. These positional vectors r, whose directions are given by the unit vector $\bar{r}$, were calculated by means of the following equations:

$$\bar{r} = -a(\bar{V}_1 + \bar{V}_2) \pm b(\bar{V}_1 \times \bar{V}_2),$$

$$b/a = \tan \Psi, \quad a^2 + b^2 = 1,$$

$$\Psi = \sin^{-1}[\sin^2\theta - \{\cos^2\theta(1 - \cos\phi)^2\}/\sin^2\phi\,]^{1/2}.$$

$\bar{V}_1$ and $\bar{V}_2$ are unit vectors between the appropriate nitrogen, carbon and cobalt atoms. θ is the Co-N-H or H-C-N bond angle, restricted to the tetrahedral angle. ϕ is the appropriate Co-N-C or C-C-N bond angle. Ψ is half the angle between the hydrogen positions. A distance of 1.036A° and 1.080A° were chosen for the N-H and C-H bond lengths respectively to give the magnitude of the r's. These calculated

Table 8. Final positional parameters for D-[$Co(en)_3$]$(NO_3)_3$[1]

	X/a	Y/b	Z/c
Co	0.1607(1)	0.2439(1)	0.7575(1)
N(1)	0.0787(5)	0.1229(5)	0.7300(11)
N(2)	0.2672(5)	0.1546(5)	0.7082(9)
N(3)	0.2503(5)	0.3607(5)	0.7673(9)
N(4)	0.0586(6)	0.3363(6)	0.8209(9)
N(5)	0.1743(5)	0.2131(6)	0.9765(9)
N(6)	0.1363(5)	0.2745(5)	0.5394(8)
N(7)	0.1492(5)	0.6019(6)	0.6455(9)
N(8)	0.2059(6)	0.8853(7)	0.8021(10)
N(9)	0.5059(6)	0.5172(6)	0.9032(11)
C(1)	0.3531(5)	0.2122(7)	0.7408(13)
C(2)	0.3361(6)	0.3268(7)	0.6927(13)
C(3)	0.0716(7)	0.3620(8)	0.9824(11)
C(4)	0.1020(7)	0.2647(8)	1.0657(11)
C(5)	0.0553(7)	0.2089(8)	0.4936(13)
C(6)	0.0620(7)	0.1049(8)	0.5654(11)
O(1)	0.1221(5)	0.5627(5)	0.7664(8)
O(2)	0.1040(5)	0.6739(5)	0.5827(9)
O(3)	0.2210(5)	0.5686(7)	0.5883(10)
O(4)	0.2343(5)	0.9556(5)	0.8915(8)
O(5)	0.2140(7)	0.7914(6)	0.8405(10)
O(6)	0.1705(7)	0.9103(6)	0.6789(9)
O(7)	0.4365(7)	0.5511(7)	0.8368(11)
O(8)	0.5645(8)	0.4661(7)	0.8343(13)
O(9)	0.5169(6)	0.5423(7)	1.0399(10)

[1]Numbers in parentheses are standard deviations in the last digit of the parameter

Table 9. Final anisotropic thermal parameters ($\times 10^5$) for D-$[Co(en)_3](NO_3)_3$ [1,2]

	β_{11}	β_{22}	β_{33}	β_{12}	β_{13}	β_{23}
Co	322(4)	428(5)	1064(12)	10(4)	-12(7)	41(10)
N(1)	408(33)	557(45)	1514(136)	-40(33)	20(58)	183(67)
N(2)	368(30)	489(39)	1476(126)	-22(30)	-32(51)	74(56)
N(3)	395(33)	576(42)	1300(113)	39(30)	100(59)	-153(66)
N(4)	405(35)	547(48)	1531(117)	28(36)	11(58)	187(62)
N(5)	446(37)	510(41)	1400(103)	59(34)	-169(53)	118(57)
N(6)	431(35)	488(44)	1102(95)	-53(30)	-143(46)	147(53)
N(7)	345(35)	677(47)	1675(133)	-48(37)	-21(61)	54(67)
N(8)	629(50)	707(60)	1725(133)	123(46)	-236(68)	27(77)
N(9)	690(54)	479(48)	1750(136)	-39(43)	80(73)	211(68)
C(1)	292(35)	727(53)	1813(151)	54(33)	-19(75)	-145(91)
C(2)	380(41)	554(52)	2151(175)	-94(42)	47(79)	-192(78)
C(3)	474(50)	735(66)	1315(134)	62(48)	24(72)	19(76)
C(4)	665(57)	652(66)	1377(121)	74(53)	186(73)	214(85)
C(5)	542(51)	759(68)	1568(153)	-65(51)	-227(74)	46(86)
C(6)	608(55)	724(64)	1442(142)	174(54)	-7(79)	-73(86)
O(1)	531(35)	776(43)	2011(123)	-42(31)	143(58)	296(70)
O(2)	632(39)	667(45)	2059(117)	66(37)	-144(61)	276(64)
O(3)	511(37)	1512(83)	1914(120)	262(47)	277(62)	433(90)
O(4)	610(41)	798(50)	1636(110)	-23(40)	-130(59)	206(64)
O(5)	1480(83)	542(43)	2880(167)	130(50)	-1078(101)	20(74)
O(6)	1076(63)	785(51)	1528(98)	225(53)	-312(81)	103(64)
O(7)	1029(61)	847(60)	2923(176)	109(56)	-651(95)	-162(87)
O(8)	1084(70)	950(65)	3824(230)	86(62)	727(113)	-383(110)
O(9)	844(53)	1054(63)	1873(135)	57(52)	-121(74)	80(89)

[1] Numbers in parentheses are standard deviations in the last digit of the parameter

[2] The form of the anisotropic temperature factor expression is $\exp[-(\beta_{11}h^2 + \beta_{22}k^2 + \beta_{33}l^2 + 2\beta_{12}hk + 2\beta_{13}hl + 2\beta_{23}kl)]$

Table 10. Observed and calculated structure factors(x10)

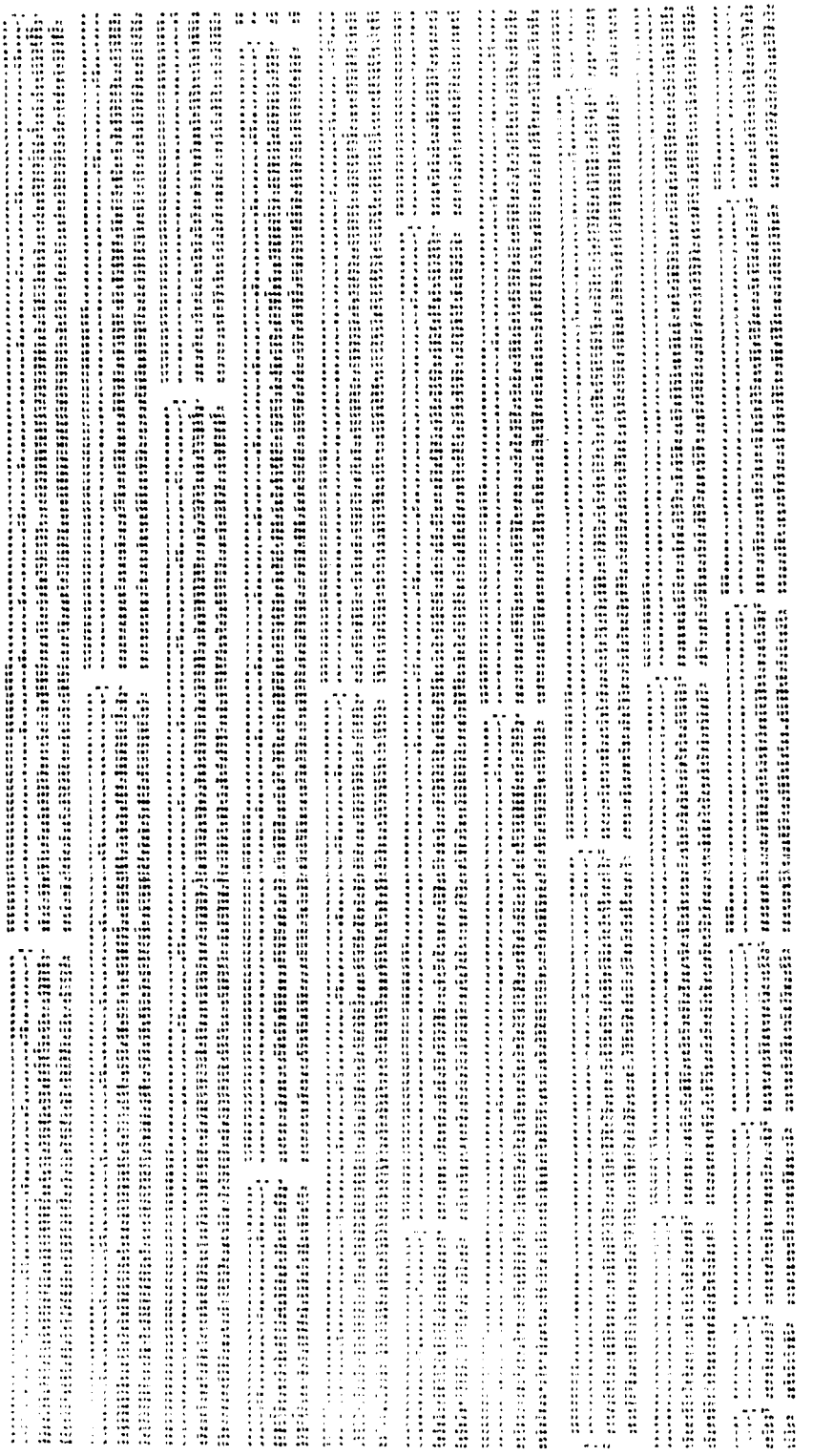

Table 11. Calculated positional parameters for hydrogen atoms

	X/a	Y/b	Z/c		X/a	Y/b	Z/c
H(N1a)	0.0169	0.1381	0.7842	H(C1a)	0.4081	0.1792	0.6732
H(N1b)	0.1086	0.0559	0.7771	H(C1b)	0.3672	0.2093	0.8618
H(N2a)	0.2652	0.1342	0.5936	H(C2a)	0.3920	0.3760	0.7320
H(N2b)	0.2649	0.0859	0.7730	H(C2b)	0.3278	0.3305	0.5702
H(N3a)	0.2635	0.3791	0.8805	H(C3a)	0.0075	0.3895	1.0300
H(N3b)	0.2241	0.4263	0.7107	H(C3b)	0.1235	0.4227	0.9932
H(N4a)	-.0029	0.2964	0.8070	H(C4a)	0.1290	0.2869	1.1761
H(N4b)	0.0599	0.4055	0.7571	H(C4b)	0.0447	0.2111	1.0778
H(N5a)	0.2379	0.2391	1.0138	H(C5a)	0.0545	0.1998	0.3710
H(N5b)	0.1718	0.1319	0.9939	H(C5b)	-.0070	0.2475	0.5302
H(N6a)	0.1928	0.2528	0.4746	H(C6a)	-.0019	0.0628	0.5508
H(N6b)	0.1206	0.3542	0.5266	H(C6b)	0.1192	0.0620	0.5169

positions were put into the least-squares program and after a few cycles values of R and ωR of 0.074 and 0.086, respectively, were obtained. A fixed isotropic temperature factor of $5A^2$ was used for the hydrogen atoms. Because some of the hydrogens were ill behaved only their calculated positions are reported.

C. X-ray and Gamma-ray Racemization

The results of the X-ray and gamma-ray racemization studies are given in Table 12. Figure 15 shows the irradiation effects on the UV-Visible absorption spectrum for the nitrate complex. Figure 16 shows the X-ray radiation induced racemization of the halide salts. From the visible absorption spectrum for these irradiated halide salts no evidence of decomposition was detectable. Figure 17 shows the X-ray induced racemization and decomposition of the nitrate salt. The slope $[d \ln(\alpha/\alpha_0)/d\ MR]$ was $(1.06 \pm .01) \times 10^{-2}\ MR^{-1}$ and the slope $[d \ln(1 - Co^{2+}/Co_t)/d\ MR]$ was $(0.16 \pm .01) \times 10^{-2}\ MR^{-1}$. This corresponded to a corrected rate for racemization of $(4.50 \pm .01) \times 10^{-3}\ MR^{-1}$. At 4680A the X-ray irradiated samples differed from the non-irradiated samples by only 8-10 percent. This corresponded to the value obtained for the formation of cobalt(II). The small change in the absorbance at 4680A could be caused by either the formation of a new cobalt species with similar extinction coefficient, to that of the nitrate complex, or to the formation of another spe-

Table 12. Results of X-ray and gamma-ray racemization studies for $[Co(en)_3]X_3$

k (MR^{-1})	Number of Data Points	Half-life (min)
X-ray[1]		
	X = Chloride•H_2O	
$(1.02 \pm .39) \times 10^{-2}$	27	5700 ± 2200
	X = Bromide	
$(5.85 \pm .06) \times 10^{-1}$	23	200 ± 20
	X = Iodide	
$(9.85 \pm .13) \times 10^{-1}$	6	120 ± 16
$(1.08 \pm .18)$	6	110 ± 18
$(9.25 \pm .05) \times 10^{-1}$	6	130 ± 7
$(9.50 \pm .04) \times 10^{-1}$	27	120 ± 5
$(9.85 \pm .24) \times 10^{-1}$	mean	120 ± 30
	X = Nitrate[2]	
$(1.05 \pm .14) \times 10^{-2}$	6	11000 ± 1400
$(0.90 \pm .04) \times 10^{-2}$	6	13000 ± 600
$(0.73 \pm .21) \times 10^{-2}$	6	16000 ± 4700
$(0.93 \pm .09) \times 10^{-2}$	18[3]	13000 ± 1100
$(0.90 \pm .03) \times 10^{-2}$	22	13000 ± 400
$(0.91 \pm .09) \times 10^{-2}$	mean[4]	13000 ± 1200
Gamma-ray[5]		
$(5.46 \pm .09) \times 10^{-4}$	6	$(3.16 \pm .06) \times 10^5$

[1]Irradiated at 50 Kvolts and a target current of 20 ma. The exposure rate was 0.36 MR/hr

[2]The k's are not corrected for decomposition

[3]The above three sets of points plotted as one set

[4]Value for last two sets

[5]The average exposure rate was 0.24 MR/hr

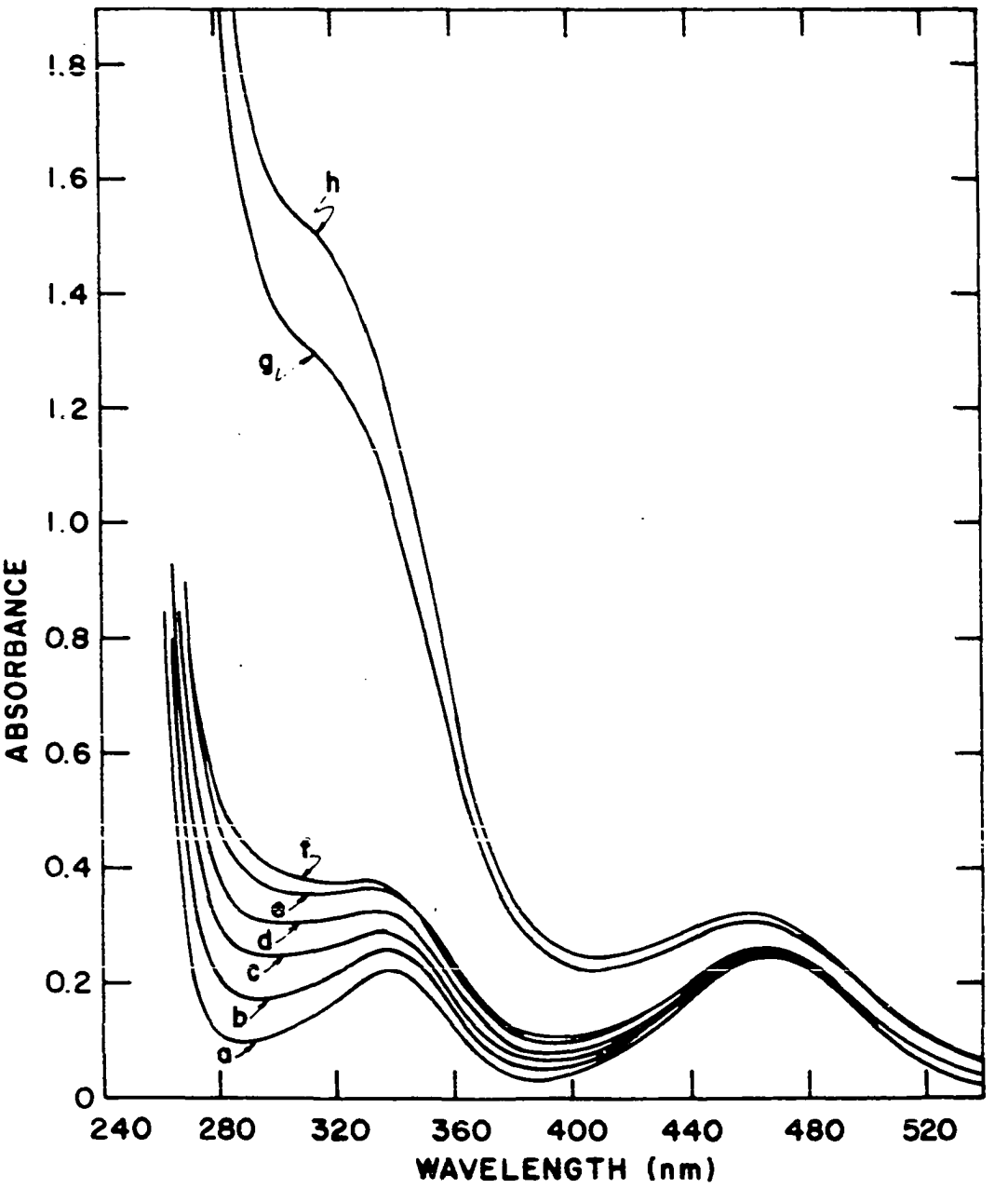

Figure 15. Radiation effects on the UV-Visible absorption spectrum for the nitrate complex. (a) Not irradiated. Irradiated with Gamma-rays: (b) 54 MR; (c) 104 MR; (d) 147 MR; (e) 185 MR; (f) 217 MR. Irradiated with X-rays: (g) 61 MR; (h) 66 MR

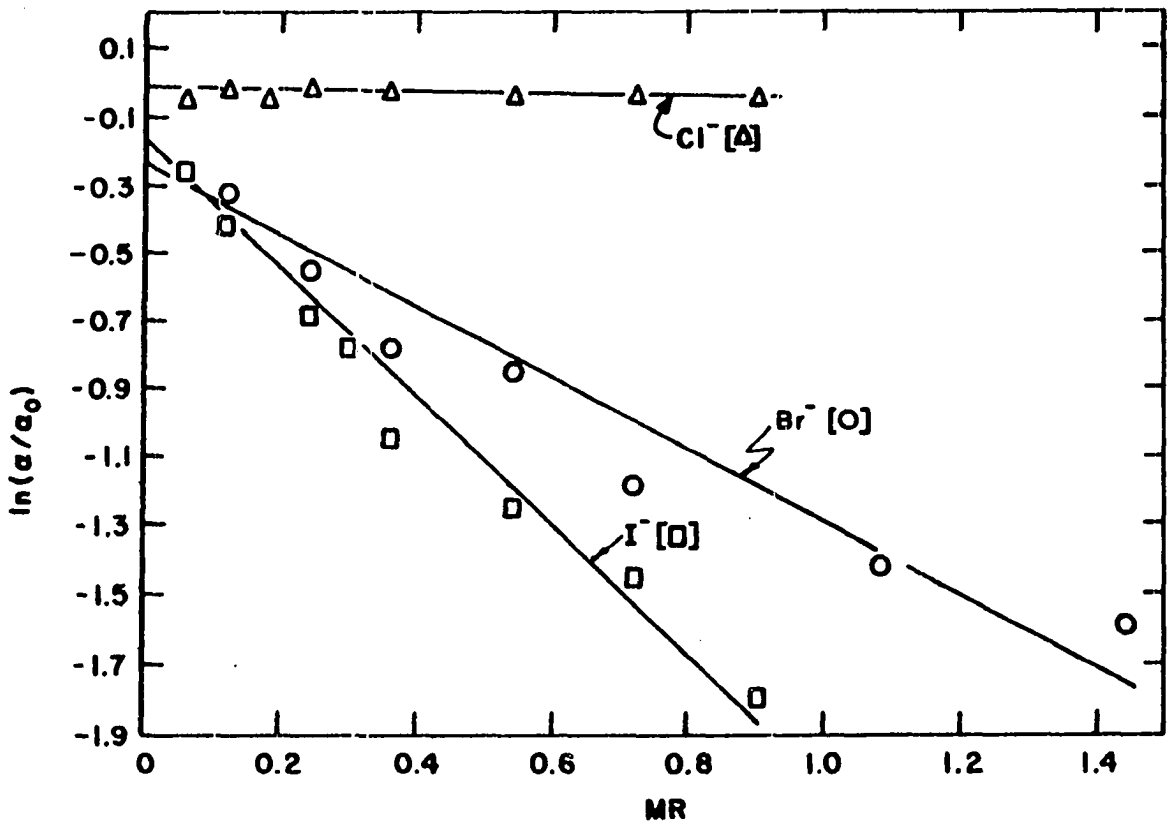

Figure 16. Racemization of the halide salts of the $[Co(en)_3]^{3+}$ ion by X-rays

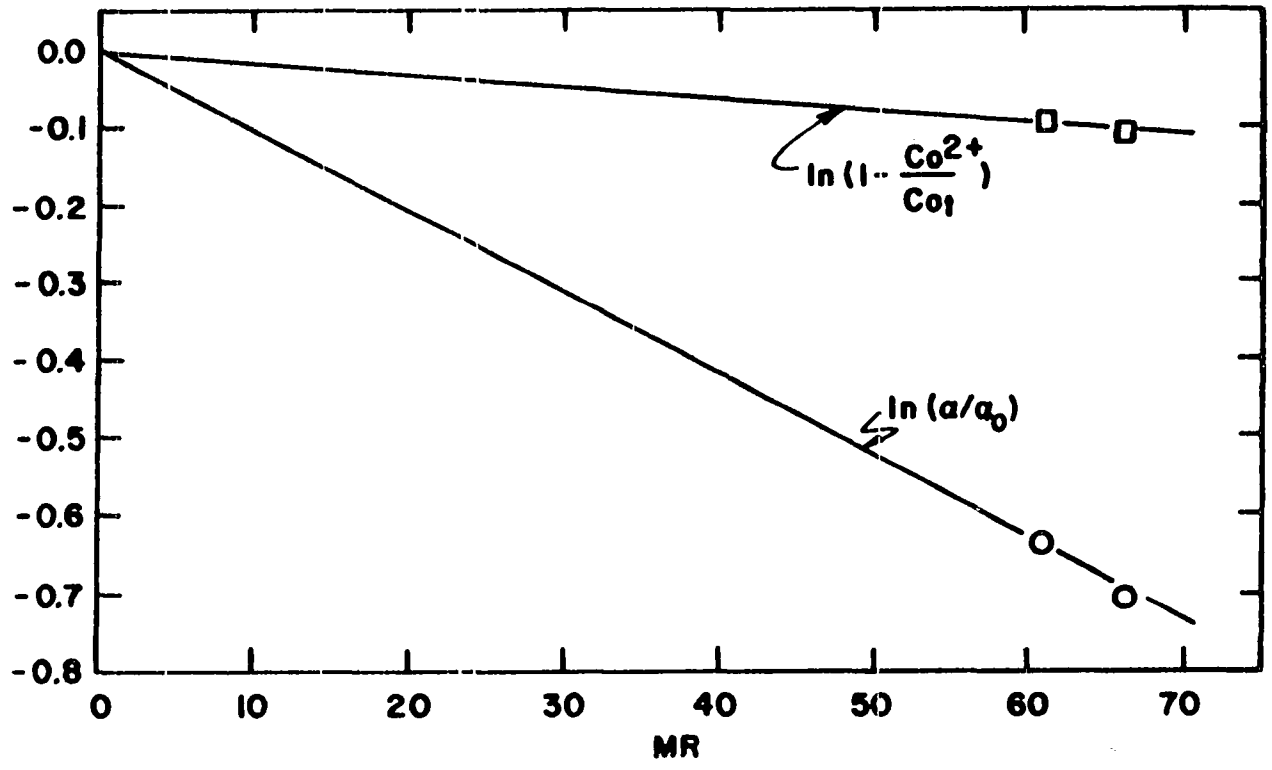

Figure 17. Loss of optical activity and decomposition of $[Co(en)_3](NO_3)_3$ by X-rays

cies in minor amounts. The voltage of the X-ray unit was 50 kvolts and the target (anode) current was 20 ma. Figure 18 shows the gamma-ray induced racemization and decomposition of the nitrate salt. The slope [d $\ln(\alpha/\alpha_o)$/d MR] was (1.01 ± .04)x10^{-3} MR^{-1} and the slope [d $\ln(1 - Co^{2+}/Co_t)$/d MR] was (3.65 ± .24)x10^{-4} MR^{-1}. This corresponded to a corrected rate for racemization of (3.20 ± .25)x10^{-4} MR^{-1}. Within the error of measurement, the absorption, at 4680A, for the different irradiations was the same.

After a sample of the nitrate complex had been irradiated with X-rays, it was noticed that upon dissolving the sample, some gas was evolved. A mass spectrum of the vapors above a frozen solution of the sample revealed one peak. This was due to hydrogen. After warming the sample to room temperature, three peaks were detected by the mass spectrometer: masses 58, 43 and 15. A high resolution mass spectrum was then obtained and the results are given in Table 13.

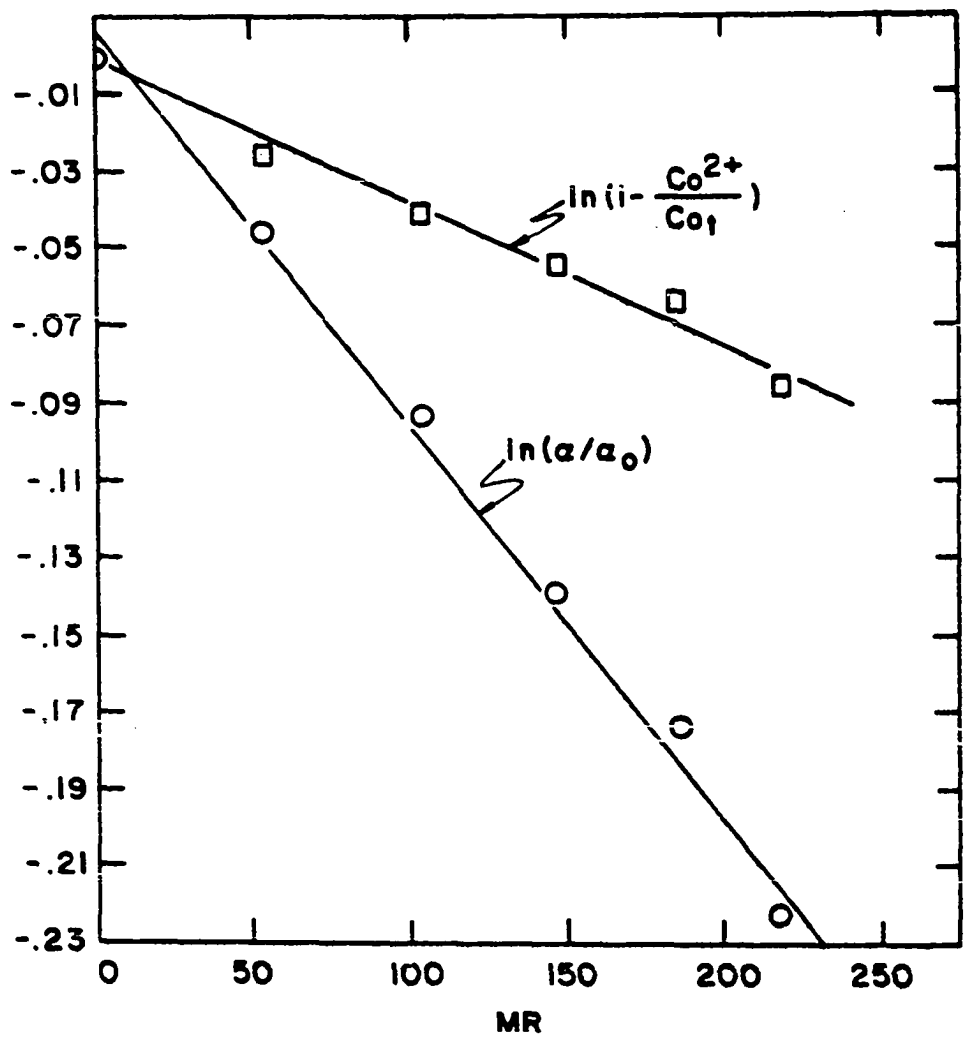

Figure 18. Loss of optical activity and decomposition of $[Co(en)_3](NO_3)_3$ by Gamma-rays

Table 13. High resolution mass spectrum of unknown gas[1]

Experimental Mass	Species	Exact Mass	Deviation
58.054484	$C_2H_6N_2$	58.053095	- 0.0014
43.028138	CH_3N_2	43.029621	+ 0.0014
15.029359	CH_3	15.023474	- 0.0059

[1]Obtained from X-ray irradiation of $[Co(en)_3](NO_3)_3$

IV. DISCUSSION

A. Thermal Racemization

From the results given in Table 7 it can be seen that the ΔH for racemization, of the halide salts, is the same within experimental error. Kutal and Bailar (12) reported that hydrated halides racemized in the following order $I^- > Br^- > Cl^-$. The ΔH for racemization of the iodide salt was the lowest, the bromide had a ΔH about four Kcal-mole^{-1} higher, but for the chloride, the ΔH for racemization lowered to a value about equal to the iodide. From the TGA analyses, the chloride salt was monohydrated, whereas the iodide, bromide and nitrate salts were anhydrous. It is therefore possible that the water of hydration, for the chloride, is playing some part in the racemization process. The ΔH for racemization of the nitrate complex is almost a factor of four greater than that of the halide salts.

The mechanism proposed for the solid-state racemization is that of a twisting mechanism, similar to those shown in Figure 3. The twisting mechanism would also explain the high ΔH of racemization for the nitrate complex. Because the nitrate group is composed of four atoms, as compared to one for the halides, it would hinder a twisting mechanism greater than would the halides. Also from the crystal structure results, to be discussed in the next section, it was shown

that there was considerable hydrogen bonding between the nitrate groups and the complex. This close interaction would prevent the molecule from undergoing faster thermal racemization, by a twist mechanism, as compared to the halide salts.

B. Crystal Structure of D-$[Co(en)_3](NO_3)_3$

Figure 19, an ORTEP drawing (39), illustrates the packing in the unit cell. (The fine lines represent the closest approach of the oxygen atoms to the hydrogen atoms attached to nitrogen atoms of the complex, out to 2.5Å). Table 14 lists some of the important interatomic distances outside the complex ion, as calculated by ORFFE (40). Figures 20 and 21 show the directions of vibration of the atoms refined anisotropically. Figure 22 shows a stereoscopic view of the complex with hydrogen atoms included.

Only one type of hydrogen bond is conceivable, that is the N-H...O bond. This occurs between the amines of the complex and the oxygen of the nitrates. The closest N...O distance is 2.913Å. This agrees with the 2.91Å reported by Iwata, Nakatzu and Saito for the N-H...O bond length in the chloride structure. They also report the shortest N-H...Cl bond length as 3.12Å. Table 15 lists the H...O bond distances and the N-H...O bond angles, as calculated by ORTEP. These distances and angles were obtained by using the calculated positions of the hydrogen atoms. There are six

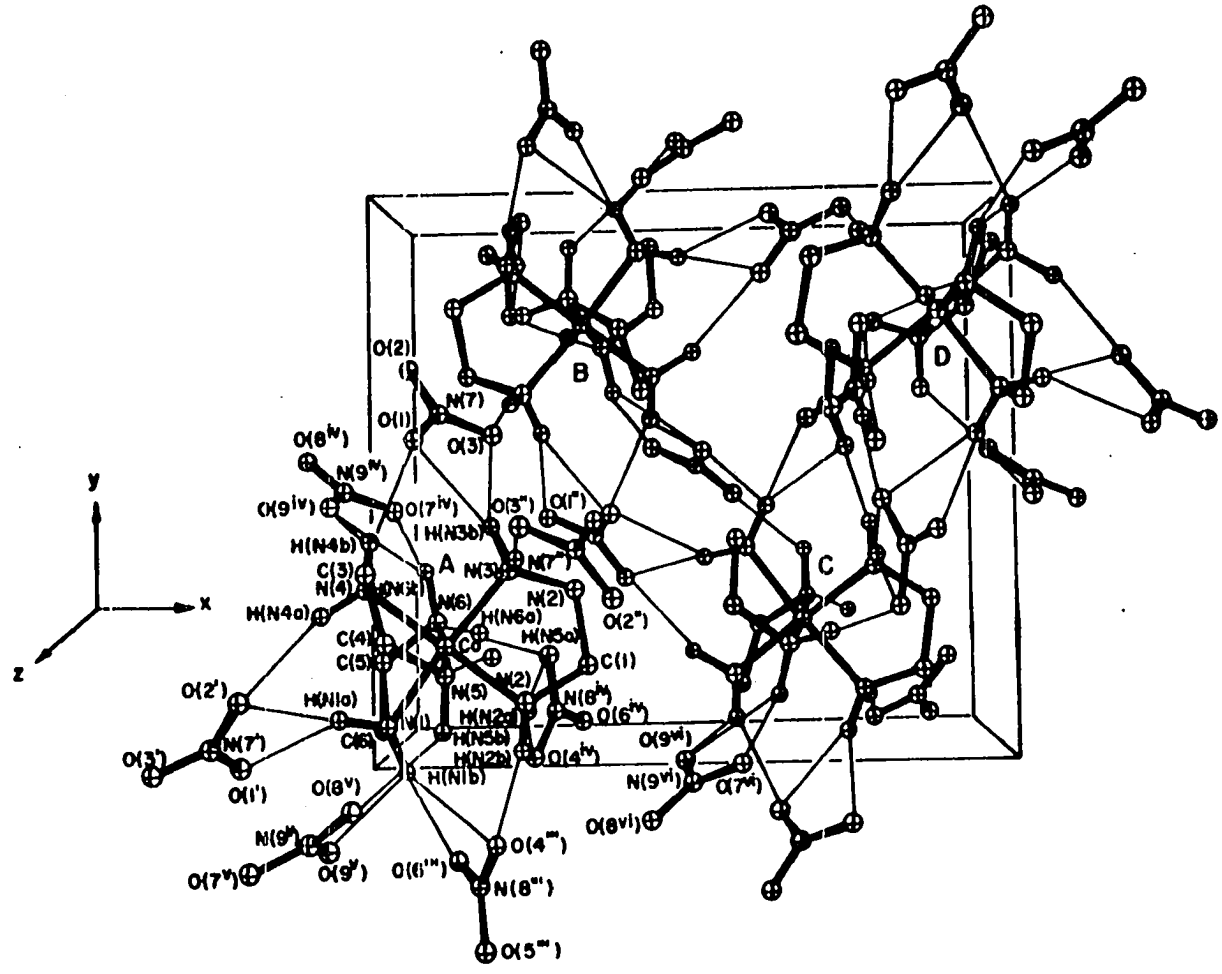

Figure 19. Packing in unit cell with fine lines indicating possible hydrogen bonding. O-H distances out to 2.5A

Table 14. Intermolecular approaches less than 3.5Å

The superscripts designate:

Symbol	x	y	z
(')	- x	y - .5	1.5 - z
('')	.5 - x	1 - y	.5 + z
(''')	.5 - x	1 - y	z
(iv)	.5 - x	1 - y	z - .5
(v)	x - .5	.5 - y	2 - z
(vi)	1 - x	y - .5	1.5 - z

Atom 1	Atom 2	Distance[1]	Atom 1	Atom 2	Distance[1]
C(1)	O(2'')	3.385(13)	N(1)	N(7')	3.479(11)
C(1)	O(8vi)	3.392(14)	N(2)	O(4''')	3.022(10)
C(1)	N(9vi)	3.436(12)	N(2)	O(4iv)	3.102(11)
C(2)	O(7)	3.421(13)[2]	N(2)	O(5iv)	3.303(12)
C(3)	O(1)	3.250(12)	N(2)	O(6''')	3.384(12)
C(3)	O(3'')	3.278(14)	N(2)	O(8vi)	3.424(13)
C(3)	O(7'')	3.287(14)[2]	N(3)	O(3'')	2.980(12)
C(4)	O(8v)	3.087(14)	N(3)	O(3)	3.084(11)
C(4)	O(3'')	3.318(15)	N(3)	O(1)	3.152(10)
C(4)	O(7'')	3.366(14)[2]	N(4)	O(1)	3.045(10)
C(4)	O(2')	3.453(14)	N(4)	O(9iv)	3.089(11)
C(5)	O(7iv)	3.326(14)	N(4)	O(2')	3.232(11)
C(5)	O(9iv)	3.332(15)	N(4)	O(6')	3.444(13)[2]
C(6)	O(6''')	3.078(14)	N(5)	O(8v)	3.214(14)
C(6)	O(1')	3.110(14)	N(5)	O(6'')	3.257(11)[2]
C(6)	O(4iv)	3.413(14)	N(5)	O(3'')	3.296(12)
N(1)	O(1')	3.009(11)	N(5)	O(4''')	3.450(12)
N(1)	O(9v)	3.034(11)	N(6)	O(5iv)	2.913(14)
N(1)	O(6''')	3.025(11)	N(6)	O(7iv)	3.016(12)
N(1)	O(2')	3.173(11)	N(6)	O(9iv)	3.201(11)
N(1)	O(4''')	3.400(10)			

[1]Numbers given in parentheses refer to standard deviations occurring in the last digit as calculated from e.s.d. given by variance-covariance matrix

[2]Not drawn

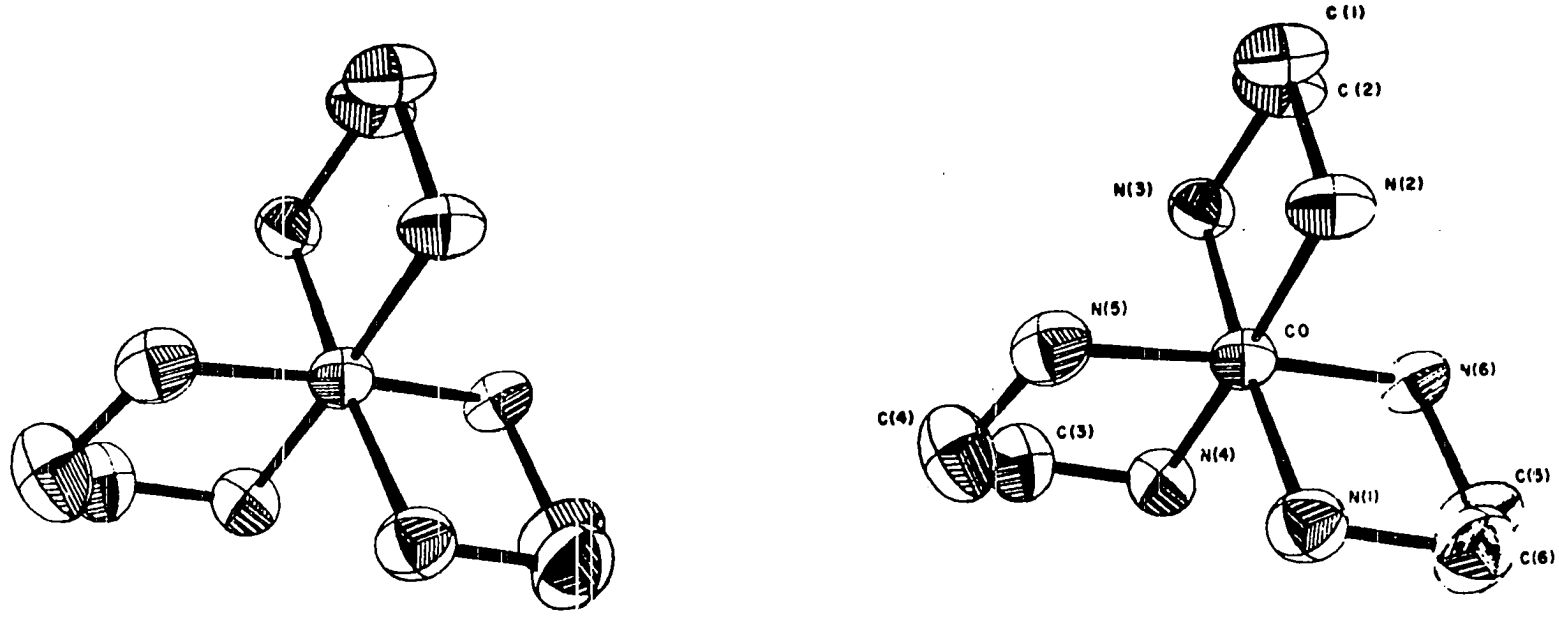

Figure 20. Stereoscopic view of the D-$[Co(en)_3]^{3+}$ moiety. Looking down the three-fold molecular axis

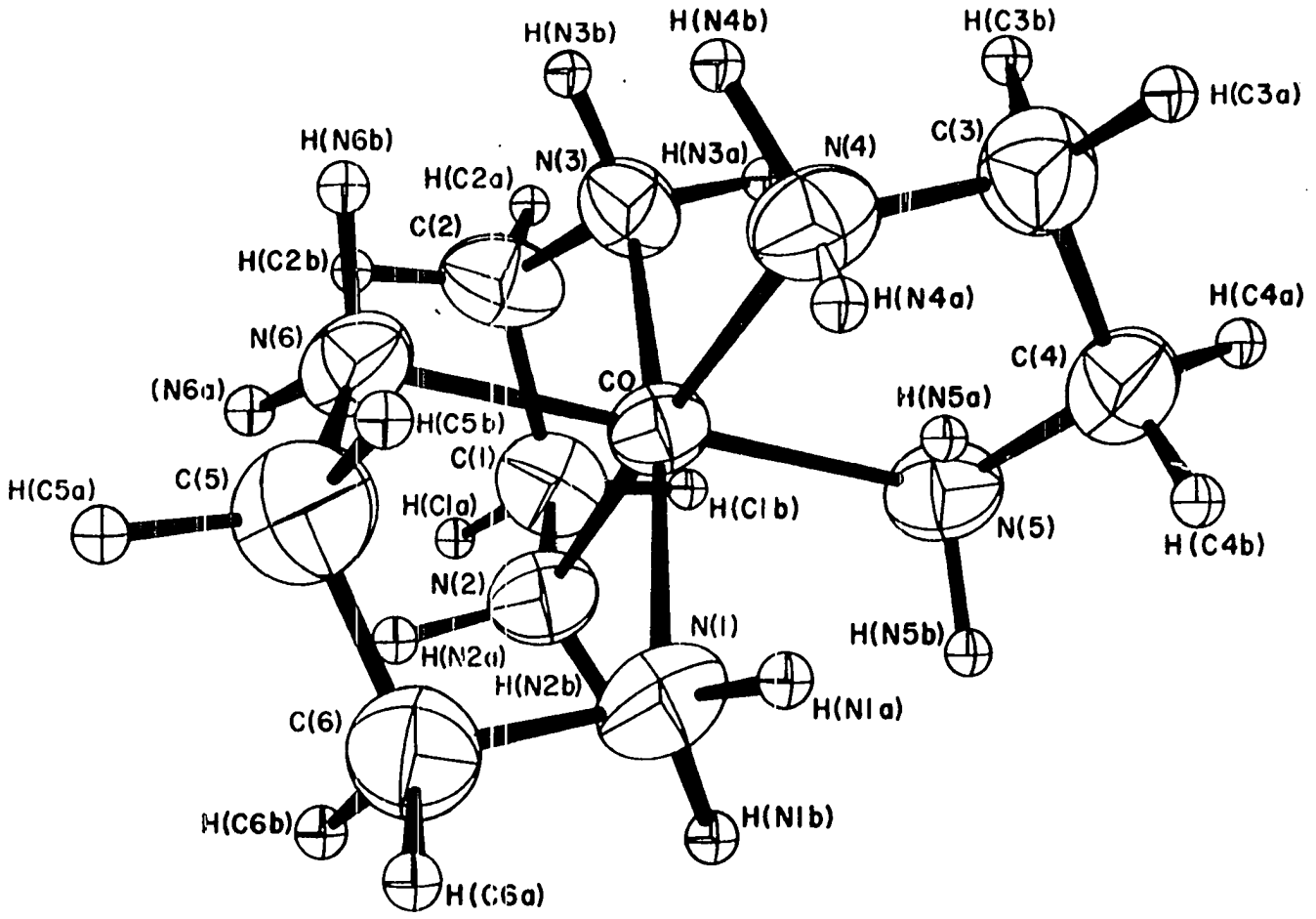

Figure 21. Unhindered view of the D-$[Co(en)_3]^{3+}$ moiety with hydrogens

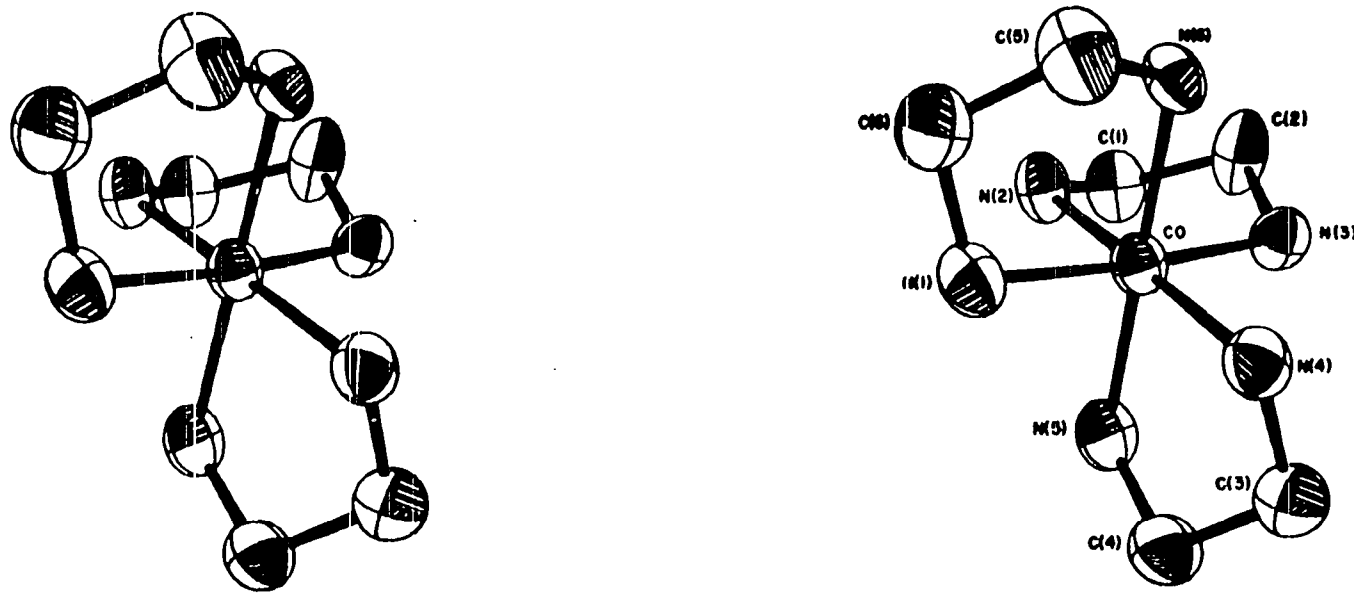

Figure 22. Stereoscopic view of the D-$[Co(en)_3]^{3+}$ moiety

Table 15. Distances and angles between calculated hydrogen positions and oxygen atoms in the nitrate groups[1]

Atom 1	Atom 2	Distance (A)[2]		Angle (deg.)
H(N1a)	O(2')	2.150	N(1)-H(N1a)-O(2')	174.2
H(N1a)	O(1')	2.269	N(1)-H(N1a)-O(1')	127.0
H(N1b)	O(6''')	2.216	N(1)-H(N1b)-O(6''')	133.7
H(N1b)	O(9v)	2.422	N(1)-H(N1b)-O(9v)	116.9
H(N1b)	O(4''')	2.432	N(1)-H(N1b)-O(4''')	154.3
H(N2a)	O(4iv)	2.101	N(2)-H(N2a)-O(4iv)	161.7
H(N2a)	O(5iv)	2.425	N(2)-H(N2a)-O(5iv)	141.8
H(N2b)	O(4''')	1.993	N(2)-H(N2b)-O(4''')	169.0
H(N3a)	O(3'')	1.949	N(3)-H(N3a)-O(3'')	172.2
H(N3b)	O(3)	2.092	N(3)-H(N3b)-O(3)	159.8
H(N3b)	O(1)	2.319	N(3)-H(N3b)-O(1)	136.4
H(N4a)	O(2')	2.336	N(4)-H(N4a)-O(2')	144.6
H(N4b)	O(1)	2.179	N(4)-H(N4b)-O(1)	138.8
H(N4b)	O(9iv)	2.299	N(4)-H(N4b)-O(9iv)	132.7
H(N5b)	O(8v)	2.491	N(5)-H(N5b)-O(8v)	126.9
H(N6a)	O(5iv)	1.874	N(6)-H(N6a)-O(5iv)	173.7
H(N6a)	O(7iv)	2.208	N(6)-H(N6b)-O(7iv)	133.5
H(N6b)	O(9iv)	2.383	N(6)-H(N6b)-O(9iv)	135.1

[1]Superscripts are listed in Table 14
[2]Distances out to 2.5A

O...H distances less than 2.15Å for each molecule or 24 per unit cell. If each of these corresponded to a hydrogen bond they could account for the added stability of the nitrate salt. Assuming 3 Kcal-mole^{-1} for a hydrogen bond this would correspond to 72 Kcal of additional stability. The N-H stretching frequency, reported by Powell and Sheppard (41), is 3195-3060 cm^{-1} for the chloride complex. The corresponding stretching frequency for the nitrate complex occurs at 3210-3110 cm^{-1}. Molecule A is related to molecules B, C, and D by screw axes located at x/4, y/2; y/4, z/2; and x/2, z/4 respectively. Additional screw axes occur at 3x/4, y/2; 3y/4, z/2; and x/2, 3z/4. The hydrogen bonding occurring between the amines of the complex and the nitrate oxygens provides for a helical relationship between the complex molecules in the unit cell.

As for the geometry of the complex, no significant change was found from the previous results of experiments with the chloride and bromide structures. Table 16 lists the interatomic distances and Table 17 the bond angles of the complex and nitrate groups. The symmetry of the complex molecule is D_3. The non-crystallographic threefold axis of rotation forms an angle of -79.5° with the x axis and 74.1° with the z axis. The six nitrogen atoms of the ligand molecules form an octahedron around the cobalt atom. The average Co-N distance is 1.964 ± 0.008Å, in good agreement with the

Table 16. Distance between atoms in complex

Atom 1	Atom 2	Distance (A)[1]
Co	N(1)	1.947(7)
Co	N(2)	1.956(7)
Co	N(3)	1.964(7)
Co	N(4)	1.967(8)
Co	N(5)	1.967(8)
Co	N(6)	1.981(7)
N(1)	C(6)	1.480(13)
N(2)	C(1)	1.468(11)
N(3)	C(2)	1.466(12)
N(4)	C(3)	1.464(12)
N(5)	C(4)	1.459(13)
N(6)	C(5)	1.489(12)
C(1)	C(2)	1.526(13)
C(3)	C(4)	1.494(14)
C(5)	C(6)	1.457(15)
N(7)	O(1)	1.233(10)
N(7)	O(2)	1.249(10)
N(7)	O(3)	1.227(11)
N(8)	O(4)	1.245(11)
N(8)	O(5)	1.236(11)
N(8)	O(6)	1.233(12)
N(9)	O(7)	1.237(12)
N(9)	O(8)	1.233(12)
N(9)	O(9)	1.249(13)

[1]Numbers given in parentheses refer to standard deviations occurring in the last digit as calculated from e.s.d. given by variance-covariance matrix

Table 17. Bond angles in complex[1]

	Angle (deg.)		Angle (deg.)
N(1)-Co-N(2)	90.31(32)	Co-N(4)-C(3)	107.65(62)
N(1)-Co-N(3)	175.69(31)	Co-N(5)-C(4)	111.29(59)
N(1)-Co-N(4)	92.49(34)	Co-N(6)-C(5)	106.99(56)
N(1)-Co-N(5)	91.70(33)	N(1)-C(6)-C(5)	106.87(86)
N(1)-Co-N(6)	85.85(30)	N(6)-C(5)-C(6)	109.47(84)
N(2)-Co-N(3)	85.15(32)	N(2)-C(1)-C(2)	106.77(67)
N(2)-Co-N(4)	175.80(34)	N(3)-C(2)-C(1)	106.64(81)
N(2)-Co-N(5)	91.15(33)	N(4)-C(3)-C(4)	108.74(86)
N(2)-Co-N(6)	92.00(32)	N(5)-C(4)-C(3)	107.99(82)
N(3)-Co-N(4)	92.16(31)	O(1)-N(7)-O(2)	120.62(92)
N(3)-Co-N(5)	91.83(32)	O(1)-N(7)-O(3)	118.86(88)
N(3)-Co-N(6)	90.81(30)	O(2)-N(7)-O(3)	120.51(94)
N(4)-Co-N(5)	85.18(32)	O(4)-N(8)-O(5)	117.95(97)
N(4)-Co-N(6)	90.74(31)	O(4)-N(8)-O(6)	120.39(97)
N(5)-Co-N(6)	175942(33)	O(5)-N(8)-O(6)	121.60(103)
Co-N(1)-C(6)	109.41(58)	O(7)-N(9)-O(8)	121.26(126)
Co-N(2)-C(1)	110.06(53)	O(7)-N(9)-O(9)	117.07(109)
Co-N(3)-C(2)	108.53(53)	O(8)-N(9)-O(9)	121.58(123)

[1]Numbers given in parentheses refer to standard deviations occurring in the last digit as calculated from e.s.d. given by variance-covariance matrix

values obtained for other $[Co(en)_3]^{3+}$ salts listed previously. The average N-Co-N angle is 89.8 ± 0.3°. Considering the combination of planes formed by three nitrogen atoms in the complex, the average position of the cobalt atom is fixed at the center of intersection of these planes. The nitrogen atoms in the nitrate groups are also planar with the oxygen atoms, within experimental error. The ethylenediamine molecules are of the gauche form, and all three C-C bonds approximately align along the non-crystallographic threefold axis of the complex, in the δδδ conformation. This conformation is opposite that predicted by Raymond, Corfield, and Ibers (42), for a strongly hydrogen-bonded system. This could be caused by bifurcation of some of the proposed hydrogen bonds. The chelate rings are not planar: C(1) and C(2) lie 0.322A above and 0.384A below the plane of Co, N(2) and N(3) respectively; C(3) and C(4) lie 0.495A above and 0.100A below the plane of Co, N(4) and N(5) respectively; C(5) and C(6) lie 0.344A below and 0.315A above the plane of Co, N(1) and N(6) respectively.

The absolute configuration of the complex was determined using the statistical method of Hamilton (43). The structure was refined anisotropically with no anomalous correction to an R value of 0.085 for the structure and its mirror image. When the anomalous correction terms were added, the R value for the structure drawn remained the same, while the R value

for the mirror image was raised to 0.089. With convergence, R values of 0.084 and 0.088 were obtained for the structure drawn and its mirror image, respectively. A right-handed coordinate system was used in all calculations and in data collection. Therefore the structure is in agreement with the criterion that the circular dichroism of the solution of this complex has a positive peak at 4930A ($\Delta\varepsilon$ = + 1.75 l-mole^{-1}-cm^{-1}) and a specific rotation at the sodium D-line of + 129°.

C. X-ray and Gamma-ray Irradiations

The rate of racemization for the halide and nitrate complexes, under the influence of X-rays follows a more logical order than the thermal racemization process. The iodide complex was the easiest to racemize, followed by the bromide, chloride and nitrate. The chloride and nitrate complexes have about the same rate constants for the racemization process. The UV-Visible spectrum of the halide salts indicated very little decomposition taking place. The maximum time used in these experiments was 150 min. for the halides. The nitrate complex was irradiated for several hours and a detectable amount of decomposition was observed. For a 184.5 hr. irradiation the nitrate complex lost 50.5% of its optical activity and analyzed for 10.3% cobalt(II).

The racemization caused by the gamma-ray irradiation was much slower than that caused by the X-ray irradiation. For a five week irradiation the sample lost 20% of its optical ac-

tivity and also underwent 8% decomposition. The lower rate constant for the gamma-ray irradiated samples, as compared to the X-ray irradiated samples, could be attributed to several reasons. One possible explanation is the different effects caused by each type of radiation. The X-rays are absorbed more readily by the cobalt atom than by the other atoms present in the complex. The gamma-rays would cause a greater reaction with the organic ligand of the complex rather than with the cobalt atom.

The mechanism for the racemization process probably differs from the twisting mechanism proposed for the thermal racemization process. Busch (44) reported the asymmetric racemization, in basic solution, of the tris(ethylenediamine)-cobalt(III) ion by using the electron transfer process described below:

$$[Co(III)en_3]^{3+} \rightleftarrows [Co(II)en_3]^{2+}$$

The cobalt(II) complex is very unstable and would racemize instantaneously. If the solution is made acidic, the cobalt(II) complex is destroyed and the reaction ends.

Because cobalt(II) and H_2 is formed in the reaction there must be some species that was oxidized. It would not seem possible for the nitrate group to be oxidized, but it is possible for the electrons to come from the oxidation of the organic species present or possibly from the oxidation of the cobalt(III) complex to a cobalt(IV) species.

It was noticed that when a sample of the X-ray irradiated material was dissolved in water it evolved some gas. The principal compound of gas given off in this process was identified as hydrogen. The solution was frozen in liquid nitrogen to prevent other species from entering the mass spectrometer. When the liquid nitrogen was removed from the solution the mass spectrum indiated the presence of another substance. The compound had three peaks, corresponding to masses 58, 43, and 15 with intensities 40, 100, and 20, respectively. Because mass 15 is such a large peak it is believed to be a distinct unit in the parent molecule. High resolution mass spectrum verified that the masses corresponded to the compositions: $C_2H_6N_2$, CH_3N_2 and CH_3 respectively. The above data would be consistent with the following molecular structures:

a) $CH_3-N=N-CH_3$ azomethane

b) $CH_3-C(:NH)NH_2$ acetamidine

c) $CH_3-CH=N-NH_2$ acetaldehyde hydrozone

d) $CH_3-CH(NHNH)$ 3-methyl diaziridine (a three-membered ring)

Structure (a) has a mass spectrum of essentially one peak corresponding to the symmetrical cleavage of the N-N double bond. Structure (b) has not been isolated in a pure form and its mass spectrum has peaks corresponding to the unknown compound, but there are several other peaks present. These ad-

ditional peaks make positive identification impossible. Structure (c) has a boiling point of 105-7°, no other information was available. Structure (d) is not known to exist, the 3,3-dimethyl and other higher derivatives are known for the three-membered ring system. The compound of mass 58 produced in the X-ray irradiation was in such small quantities that positive identification was impossible.

If the $[Cd(en)]^{2+}$ complex, which is known to be a bridged species (45), is irradiated with X-rays, the resulting mass spectrum contained several low molecular weight masses, the intensity of the peaks were very small. None of the masses were 58, 43 or 15. The work on the cadmium complex indicated that the nitrogen atoms have to be coordinated to the same central metal atom.

The mass spectrum of a solution of the gamma-ray irradiated sample indicated several peaks of masses 44 and below. The mass 44 peak had the largest intensity. It was believed that this mass spectrum was that of a mixture and no further identification was tried.

V. FUTURE WORK

Out of the irradiation studies have arisen several interesting problems for further investigation, also the possibility of some practical uses for the above research work. Some of these ideas are listed below:

a) Irradiation of other amine complexes (i.e. pn, bn, edta, etc.)

b) Irradiation of other coordinating ligands (i.e. acac, ox, and possibly some sulfur containing ligands)

c) Studies using different metals as the coordinating center atom

d) Use of specific wavelength radiation in the X-ray and gamma-ray irradiations

e) The use of the nitrate complex as a radiation monitoring device for high exposure rates.

Additional techniques which might prove useful for separating and identifying small quantities are column chromatography using specific absorbing resins and also the use of GC-Mass Spec.

VI. LITERATURE CITED

1. Piper, T. S., J. Am. Chem. Soc., 83, 3908 (1961).

2. Jensen, K. A., Inorg. Chem., 9, 1 (1970).

3. Ray, P. and Dutt, N. K., J. Indian Chem. Soc., 20, 81 (1943).

4. Bailar, J. C., Jr., J. Inorg. and Nucl. Chem., 8, 165 (1958).

5. Gehman, W. G., Ph.D. Thesis, Pennsylvania State University, State College, Pa., 1954.

6. Seiden, L., Ph.D. Thesis, Northwestern University, Evanston, Ill., 1957.

7. Eisenberg, R. E. and Ibers, J. A., Inorg. Chem., 5, 411 (1966).

8. Springer, C. S., Jr. and Sievers, R. E., Inorg. Chem., 6,852 (1967).

9. Gillard, R. D., "Progress in Inorganic Chemistry," Vol. 7, Cotton, F. A., ed., John Wiley and Sons, Inc., New York, N. Y., 1966, pp 247-255.

10. Saito, Y., Nakatsu, K., Shiro, M. and Kuroya, H., Bull. Chem. Soc. Japan, 30, 795 (1957).

11. LeMay, H. E. and Bailar, J. C., Jr., J. Amer. Chem. Soc., 90, 1729 (1958).

12. Kutal, C. R. and Bailar, J. C., Jr., J. Phys. Chem., 76, 119 (1972).

13. Kutal, C. R., Ph.D. Thesis, University of Illinois, Urbana, Ill., 1970.

14. Iwata, M, Nakatzu, K. and Saito, Y., Acta Cryst., B25, 2562 (1969).

15. Nakatsu, K., Bull. Soc. Japan, 35, 832 (1962).

16. Johnson, D. A. and Sharpe, A. G., J. Chem. Soc., 3490 (1964).

17. Hin-Fat, L. and Higginson, W. C. E., J. Chem. Soc. A, 298 (1967).

18. Bjerrum, J., "Metal Ammine Formation in Aqueous Solutions," Hause, Copenhagen, Denmark, 1941.

19. Klein, D., Moeller, C. W. and Ward, R., J. Amer. Chem. Soc., 80, 265 (1958).

20. Balog, J., Csaszar, J. and Kiss, L., Acta Chim. Acad. Sci. Hung., 33, 77 (1962).

21. Klein, D. and Moeller, C. W., Inorg. Chem., 4, 394 (1965).

22. Taylor, W. C., Jr. and Moeller, C. W., Inorg. Chem., 4, 398 (1965).

23. Spees, S. T. and Adamson, A. W., Inorg. Chem., 1, 531 (1962).

24. Katakis, D. and Allen, A. O., J. Phys. Chem., 68, 1359 (1964).

25. Neokladnova, L. N. and Shagisultanova, G. A., Akademiia Nauk, SSSR Doklady Chemistry, 148-153, 329 (1963).

26. Svec, H. J. and Flesch, G. D., J. Mass. Spec. and Ion Phys., 1, 41 (1968).

27. Broomhead, J. A., Dwyer, F. P. and Holgrath, J. W., "Inorganic Systhesis," Vol. 6, Rochow, E. G., ed., McGraw-Hill Book Company, Inc., New York, N. Y., 1960, pp 183-186.

28. Werner, A., Ber., 45, 121 (1912).

29. Davies, M. and Parsons, A. E., Chem. and Ind., 628 (1958).

30. Sandell, E. B., "Colorimetric Determination of Traces of Metals," 3rd ed., Interscience Publishers, Inc., New York, N. Y., 1959.

31. Hughes, R. G., Endicott, J. F., Hoffman, M. Z. and House, D. A., J. Chem. Ed. 440 (1969).

32. Clinical Dosimetry: Recommendations of the International Commission on Radiological Units and Measurements. ICRU Report 10d. National Bureau of Standards Handbook No. 87, 1962.

33. Cameron, J. R., Suntharalingam, N. and Kenney, G. N., "Thermoluminescent Dosimetry," The University of Wisconsin Press, Madison, Wis., 1968.

34. Weiss, J., Allen, A. O. and Schwarz, H. A., Proc. Intern. Conf. Peaceful Uses of Atomic Energy, Geneva, 1955, 14, 179, United Nations, New York, 1956.

35. Alexander, L. E. and Smith, G. S., Acta Cryst., 15, 983 (1962).

36. Williams, D. E. and Rundle, R. E., J. Amer. Chem. Soc., 86, 1660 (1964).

37. Doyle, P. A. and Turner, P. S., Acta Cryst., A24, 390 (1968).

38. Cromer, D. T. and Liberman, D., J. Chem. Phys., 53, 1891 (1970).

39. Johnson, C. K., ORTEP, Report ORNL-3794, Oak Ridge National Laboratory, Oak Ridge, Tenn., 1965.

40. Busing, W. R., Martin, K. O. and Levy, H. A., ORFFE, Report ORNL-TM-306, Oak Ridge National Laboratory, Oak Ridge, Tenn., 1964.

41. Powell, D. B. and Sheppard, N., J. Chem. Soc., 791 (1959).

42. Raymond, K. N., Corfield, P. W. R. and Ibers, J. A., J. Inorg. Chem., 7, 842 (1968).

43. Hamilton, W. C., Acta Cryst., 18, 502 (1965).

44. Busch, D. H., J. Amer. Chem. Soc. 77, 2747 (1955).

45. Iwamoto, T. and Shriver, D. F., Inorg. Chem., 10, 2428 (1971).

VII. ACKNOWLEDGEMENT

The author wishes to express his gratitude to Dr. Don S. Martin for his advice, encouragement and the many helpful suggestions given during the course of this research.

Appreciation is also expressed to Dr. Harry J. Svec, Gerald Flesch and Keith Cherry for their cooperation in doing the mass spectral analyses.

Appreciation is also expressed to Dr. Robert A. Jacobson, Dr. Jon C. Clardy, John E. Johnson, Wolfgang Pflaum and Camden Hubbard for their assistance in solving the crystal structure of the nitrate complex and special thanks to Dr. Jacobson for allowing me the use of his X-ray facility for the irradiation studies.

Appreciation is also expressed to Joseph Crudele and Marvino Hill for their cooperation in the gamma-ray studies.

Appreciation is also expressed to John Richards for use of the TGA apparatus.

Finally I would like to express appreciation to my wife who has been very helpful in proofing this manuscript.